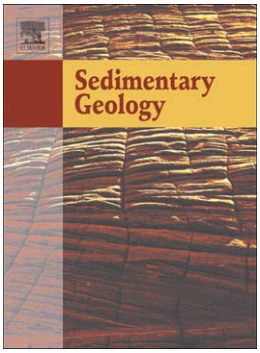

Diagenesis and fracturing of a large-scale, syntectonic carbonate platform

Hamed A. Arosi, Moyra E.J. Wilson

PII: S0037-0738(15)00147-5
DOI: doi: 10.1016/j.sedgeo.2015.06.010
Reference: SEDGEO 4875

To appear in: *Sedimentary Geology*

Received date: 13 March 2015
Revised date: 21 June 2015
Accepted date: 22 June 2015

Please cite this article as: Arosi, Hamed A., Wilson, Moyra E.J., Diagenesis and fracturing of a large-scale, syntectonic carbonate platform, *Sedimentary Geology* (2015), doi: 10.1016/j.sedgeo.2015.06.010

Diagenesis and fracturing of a large-scale, syntectonic carbonate platform.

Hamed A. Arosi and Moyra E.J. Wilson

Department of Applied Geology, Curtin University, GPO Box U1987, Perth, Western Australia 6845, Australia.

E-mails: h.arosi@postgrad.curtin.edu.au, m.wilson@curtin.edu.au

Keywords: Cenozoic, syntectonic carbonate platform, marine, meteoric and burial diagenesis, Sulawesi in equatorial SE Asia, fracturing

Abstract

The influence of coeval tectonics on carbonate platform development is widely documented, yet the diagenesis of such syntectonic platforms is barely evaluated. An outcrop, petrographic and geochemical study details here for the first time the diagenesis of the Tonasa Limestone developed in an extensional regime in central Indonesia. This equatorial carbonate system was affected by block faulting, tilt-block rotation, differential uplift and subsidence throughout its Eocene to Early Miocene history (Wilson, 1999; Wilson et al., 2000). The Tonasa carbonate platform is dominated by alteration in shallow to deeper burial depths by fluids with predominantly marine precursor origins. Mechanical and chemical compaction features are common, as are a range of mainly burial-related granular mosaic, blocky and equant calcite cements. Earlier marine cements and meteoric influences are rare, being highly localised to block faulted highs and/or bathymetrically upstanding platform margin areas. Early marine micritisation of

allochems was common on the platform top. Tectonic uplift together with a major oceanic throughflow current are thought to be key influences on localised karstification, meteoric diagenesis and marine cementation. The distribution and orientation of faults, fractures and calcite veins together with evidence for their relative timing are the strongest manifestation of tectonism coeval with diagenesis. There is concordance in the orientation and timing of structures affecting the Tonasa Platform with those basin-wide, with the potential for reactivation of pre-existing basement fabrics. Tectonic subsidence, including fault-associated differential subsidence, controlled the degree of burial diagenesis impacting different areas of the platform. A predominance of burial diagenetic features and dearth of earlier marine or meteoric cementation is seen in other Tertiary equatorial platforms and is partly attributed to: (1) predominance of non-framework building larger benthic foraminifera and/or algae that are prone to remobilisation, have low production rates and limited potential to build to sea level, and (2) high runoff due to the equatorial humid climate contributing to lowered marine salinities in SE Asia. Underlying tectonic reasons for the preponderance of a "regional" diagenetic signature over a "syntectonic" one, fracturing excepted, are: (1) development on the flanks of a backarc basin not on typical continental crust, (2) key platform influencing structures are oblique to the main extensional direction in the basin, and (3) development in an overall subsiding tectonic regime, post-dating basin initiation. The aim here is that this study will contribute to understanding diagenetic alteration of syntectonic carbonate platforms, and those from equatorial regions.

Introduction

The development of syntectonic carbonate platforms from a range of tectonic regimes is widely documented in the literature (Burchette, 1988; Gawthorpe et al., 1994; Dorobek, 1995; 2008a; 2008b; Wilson et al., 2000; Wilson and Hall, 2010), yet the diagenesis of such platforms is poorly detailed. In the active tectonic area of SE Asia at least two-thirds of the isolated carbonate platforms are documented to have formed over faulted antecedent highs with carbonate accumulation on many of these platforms coeval with local continued tectonism; i.e., many are syntectonic (Wilson and Hall, 2010). Isolated systems in SE Asia contain 83% of the hydrocarbon reserves within the regions carbonates. With many of these platforms being tectonically influenced there is an economic driver to better understand the variable diagenesis of syntectonic platforms and any impact on reservoir potential (Wilson and Hall, 2010). Tectonics may influence carbonate systems through uplift, differential subsidence, or active faulting (Burchette, 1988; Wilson and Hall, 2010). Localised uplift and karstification of footwall highs and significant local variations in stratal thicknesses across platforms have all been documented for syntectonic carbonate platforms (Burchette, 1988; Rosales et al., 1994; Wilson, 1999; Wilson et al., 2000; Bachtel et al., 2004). The diagenetic details, or implications for platform alteration, of these localised karstic features or stratal thickening are generally not discussed (Rosales et al., 1994). Various studies have detailed fracture patterns in carbonate systems, but these are rarely linked to syntectonic sedimentation, and the diagenesis of such fractures remains underevaluated (Rosales et al., 1994; Cloke et al., 1999a; Van Geet et al., 2002; Breesch et al., 2009). The climatic, oceanographic and basinal context unique to any platform will also influence platform alteration and these factors may be indirectly affected by tectonics (Moore, 2001; Wilson, 2012). The major question addressed here is: to what extent does

the tectonic regime influence the diagenesis of syntectonic platforms, or are regional or basinal controls more influential on the alteration of such systems?

The Eocene to Miocene Tonasa Carbonate Platform of Sulawesi, Central Indonesia is a well-documented syntectonic platform for which the influences on diagenesis of: (1) tectonics, (2) an equatorial climatic setting and (3) basin context are detailed here for the first time. Plate tectonic drift and associated changes in carbonate communities and their alteration is an additional influence on carbonate platform development (Davies et al., 1989) and diagenesis that is not documented here.

The sedimentology and evolution of the Tonasa Carbonate Platform have been previously documented, with inferred dominant controls on deposition including tectonics, volcanism, nutrients and oceanography (Wilson, 1996; 1999; 2000; Wilson and Bosence, 1996; 1997; Wilson et al., 2000; Wilson and Vecsei, 2005). However, there has been almost no prior diagenetic analysis of the Tonasa Limestone, with just minor mention of reservoir quality issues (Wilson, 1996; 2000; Wilson and Bosence, 1997). The previous sedimentary studies set the context for this diagenetic evaluation. Diagenetic "interactions" between the carbonates of the Tonasa Formation and the overlying and intruding igneous strata are the subject of a further study (Arosi et al., in prep.).

Geological Setting

Sulawesi, including the Tonasa Formation of this study, is located in the centre of the Indonesian Archipelago in the midst of one of the most complex, active tectonic regions in the world (Fig. 1; Hamilton, 1979; Hall, 1996, 2002a; Hall and Wilson, 2000; Hall et al., 2011). From the Mesozoic, and throughout the Cenozoic,

SE Asia has been affected by the interaction of three main tectonic plates the: Pacific-Philippine, Indo-Australian and Eurasian plates (Hamilton, 1979; Daly et al., 1991; Hall and Wilson, 2000). Hall (2002a) outlined three main collisional tectonic events at 45, 25 and 5 Ma that resulted in tectonic 'reorganisation' within SE Asia.

The evolution of south western Sulawesi (the South Arm) during the late Mesozoic and Cenozoic is linked to the accretion of micro-continental and oceanic fragments onto the eastern margin of the comparatively stable Eurasian plate, together with backarc rifting and volcanic arc development (Sukamto, 1975; Hamilton, 1979; van Leeuwen, 1981; Wilson and Bosence, 1997, Wilson, 1999, 2000). Relatively complete, but very different Late Cretaceous to recent stratigraphic sequences in the western and eastern halves of the South Arm reflect this complex geological evolution (Fig. 2; van Leeuwen, 1981; Wilson, 1999). The Balangbaru and Marada Formations are deep-marine forearc clastics and shales of Late Cretaceous age that overlie intersliced metamorphic, ultrabasic and sedimentary basement lithologies in the western South Arm (van Leeuwen, 1981; Hasan, 1991). By the Eocene, subduction had shifted to the east and marginal marine siliciclastics of the Malawa Formation in western South Sulawesi are associated with rifting of a broad basinal area centred on the Makassar Straits. The clastics pass transgressively upwards to carbonates of the Eocene to Miocene Tonasa Formation of this study that have predominantly shallow-water origins. During the Tertiary, accumulation of sedimentary rocks predominated in western South Sulawesi, whereas volcanic and igneous lithologies dominated to the east. This east-west lithological subdivision occurs across a major structural divide, today demarked by the fault-bounded, NNW-SSE trending Walanae Depression (Fig.

2). The varied igneous rocks of eastern South Sulawesi include arc-related volcaniclastics, passive margin volcanics associated with the cessation of subduction, potassic volcanics linked to extension, as well as MORB-like volcanics from an accreted transtensional marginal oceanic basin (Sukamto 1982; Yuwono et al. 1987; van Leeuwen et al., 2010). Middle to late Miocene volcaniclastics and volcanics of the Camba Formation overlie the Tonasa Formation (Sukamto, 1982; Yuwono et al. 1987; Wilson, 2000). The Miocene shift in volcanism to western South Sulawesi and associated potassic igneous intrusions are linked to microcontinental collision related volcanism and post-collisional magmas (Elburg and Foden, 1999; Elburg et al., 2003).

Deposition and development of the Tonasa Formation

The Early or Middle Eocene to Middle Miocene Tonasa Formation of this study comprises the main part of the Tertiary succession in the western part of South Sulawesi. The formation consists of shallow carbonate platform, associated slope and adjacent bathyal deposits that locally crop out over a 160 by 80 km north-south and east-west extent, respectively (Figs. 2, 3 and 4; Wilson and Bosence, 1996; 1997). Previous studies on the sedimentology and evolution of the Tonasa Carbonate Platform, together with evaluations of controlling influences set the context for this diagenetic study, and are briefly outlined below (Wilson, 1996; 1999; 2000; Wilson and Bosence, 1996; 1997; Wilson et al., 2000; Wilson and Vecsei, 2005).

Shallow-water deposits of the Tonasa Carbonate Platform are mainly wackestone, packstones and grain/rudstones that are dominated by larger benthic

foraminifera. Other components include small benthic foraminifera, echinoid remains, coralline algae and more rarely corals (Wilson and Bosence, 1997; Wilson and Rosen, 1998; Wilson et al., 2000). Planktonic foraminifera are abundant in basinal marls. The marls interdigitate with slope and platform-fringing breccias and pack/grain/rudstones. The slope deposits contain abundant shallow-water bioclasts that were reworked downslope as well as a range of lithic clasts derived from the Tonasa and underlying formations (Wilson and Bosence, 1996; Wilson, 1999; Wilson et al., 2000).

Carbonate sedimentation of the Tonasa Formation began diachronously, with shallow-water deposits forming earliest in the northern Barru and southern Jeneponto Areas during the Early to Middle Eocene (Fig. 2; Wilson et al., 2000). By the Late Eocene shallow carbonate sedimentation had spread across much of western South Sulawesi. However, during the latter part of the Late Eocene fault segmentation resulted in rapid localised deepening and drowning of the platform in the northern Barru, eastern Segeri and westerly Western Divide Mountains Areas (Fig. 2; Wilson, 1999; Wilson et al., 2000). Some of the faults including those bounding the northern and eastern extent of main shallow platform development are linked to major structural divides. These occur along strike from the NW-SE trending Adang Fault and as bounding faults to the NNW-SSE trending fault-bounded graben of the Walanae Depression, with potential involvement and reactivation of earlier basement structures (Figs. 1 and 2; van Leeuwen, 1981; Wilson and Bosence, 1996; Wilson et al., 2000). A large-scale (100 km north to south) tilted-fault-block platform with a segmented faulted northern margin (northern Barru Area) and gently dipping southern margin (southern Jeneponto Area) accumulated over 600 m of shallow water platform carbonates centred on

the central Pangkajene Area (Wilson et al., 2000). Although onshore volcaniclastics cover parts of the more southerly deposits of this platform, in the area directly offshore to the west seismic data reveals the unbroken north to south nature of the coeval continuation of the platform (Letouzey et al., 1990). Up to 1100 m of shallow and mainly deep-water carbonates accumulated to the north (Barru) and south (Jeneponto) of the main platform. Areas of more complex faulting to the east and west of the main platform resulted in localised fault-block platforms and intervening small-scale basinal grabens (western Segeri and eastern Western Divide Mountains Areas on Fig. 2; Wilson et al., 2000; Wilson, 2000). Major shallow-water facies belts on the main tilt-block platform trend E-W, were aggradational and remained static through time. Low to moderate energy wackestones and packstones dominated in the north and south of the main shallow-water tilt-block platform, whereas higher energy grainstones prevailed in the central facies belt (Wilson and Bosence, 1997; Wilson et al., 2000). Water depths and energy, linked to differential subsidence/uplift together with the presence/absence of shallow shoaling protective 'barriers' along the westerly windward platform margin, are inferred to be important influences on the facies and biota present (Wilson and Bosence, 1997; Wilson et al., 2000). Localised subaerial exposure is inferred for the shallowest part of the main tilt-block platform on the northerly footwall high and also for some of the east-west developed block-faulted platforms (Wilson and Bosence, 1996; 1997; Wilson et al., 2000; Wilson, 2000). Mass reworking of material was common from the faulted highs into adjacent basinal graben and is often linked to phases of tectonic activity (Wilson and Bosence, 1996; Wilson, 1999; Wilson, 2000; Wilson et al., 2000). On the gently dipping southern hangingwall slope of the main tilt-block platform there

was southward progradation of ramp deposits into bathyal areas during periods of tectonic quiescence and minimal subsidence (Wilson and Bosence, 1997; Wilson et al., 2000). Final demise of the platform at the end of the Early Miocene was linked to a laterally variable combination of fault-related drowning, uplift and subaerial exposure together with smothering by volcaniclastics (Wilson, 2000).

Methods

Carbonates of the Tonasa Formation are exposed as massive karstic outcrops up to 700 m high and in low riverbank exposures in western South Sulawesi. Good exposure allowed high resolution sampling, sedimentary logging, facies mapping and partial section correlation throughout the shallow water platform and adjacent basinal deposits. Eighty-one measured sections were logged (totaling >7 km of section) and of the ~1200 samples collected ~500 were thin sectioned or made into acetate peels. A subset of 153 representative thin sectioned samples that covered the full range of diagenetic features observed in the Tonasa Formation from 26 key sections were evaluated for this diagenetic study. As reported in Wilson et al. (2000) age assignments of samples were through comparison with the modified East India Letter Classification for larger benthic foraminifera (van der Vlerk and Umbgrove, 1927; Adams, 1970; Lunt and Allan, 2004) correlated against the 2004 geological timescale of Gradstein et al (Figs. 3 and 4).

Lithological components, microfacies, diagenetic phases and the relative timing of diagenetic events were determined through thin-section petrography.

All samples were half stained with Alizarin Red S and potassium ferricyanide to allow identification of dolomite, ferroan and non-ferroan calcite (Dickson, 1965, 1966). The relative abundance of components and diagenetic phases were recorded semi-quantitatively (visual estimates; after Mazzullo and Graham, 1988). Facies nomenclature follows the textural classification scheme of Dunham (1962), modified by Embry and Klovan (1971), with components given in lithology names where they exceed 10-15%. Nomenclature on carbonate cement morphologies follows Flügel (2004). Cold cathodoluminescent (CL) microscopy study of 32 polished sections was via a Technosyn 8200 MkII luminoscope (after Witkowski et al., 2000). Samples for CL analysis were selected to investigate the range of coarse (>250 μm) cement phases present.

Stable-isotope analysis ($\delta^{18}O$ and $\delta^{13}C$) was undertaken on 36 samples micro-drilled from the rock off-cut counterpart of the thin sections. Drilling sites matched directly to the off-cuts, correspond to a range of depositional and diagenetic features identified in thin section. Drilled samples include bioclasts, matrix and a range of cements with varied morphologies, with the later including those filling fractures. Oxygen and carbon isotope analyses were run on a VG Isocarb automated system online to a VG Isogas Prism II isotope-ratio mass spectrometer. All data have been normalised, to NBS-19: a primary carbonate standard used to define the V-PDB scale ($\delta^{13}C$ = +1.95‰, $\delta^{18}O$ = -2.2‰). In addition, replicate analyses of an internal carbonate standard (Mab2b) were reproducible to ±0.1‰.

Fractures were recorded in four ways to evaluate their orientations, and to gauge their potential relative timing with respect to carbonate sedimentation. (1) The strike orientations, and where possible dip data, for large-scale faults was recorded from field observations and the geological maps of South Sulawesi (scale: 1:250,000; Sukamto, 1982; Sukamto and Supriatna, 1982). (2) Strike and dip data were measured for millimetre to centimetre-scale aperture fractures, calcite veins (and joints) seen in outcrop during fieldwork. These small-scale features will have likely been under-recorded in all areas due to masking by heavy dripstone coating on the upstanding karstic outcrops and an algal film and/or up to 2 cm tufa-like coating on low river outcrops. (3) In thin sections, the ratio of numbers of both highly irregular and straight fractures to numbers of samples studied were recorded from key sections of all ages through *in situ* shallow platform and deeper slope to basinal deposits in all areas. Whilst not diagnostic, the highly irregular fracturing is more likely to have occurred when the deposits were semi-lithified, as opposed to fully lithified for the straight fractures. (4) In the slope breccia deposits consisting of material reworked into deeper water settings the ratio of numbers of both fractures and/or calcite filled veins constrained to within lithic clasts and those that cross-cut multiple clasts within the breccia fabric were recorded versus the number of samples studied. This latter data was recorded from thin sections through breccia units with lithic clasts of at least 5 mm across from the northern, western and eastern areas where these deposits range from Late Eocene to Miocene in age (cf. Wilson and Bosence, 1996; Wilson et al., 2000). Fractures within clasts, commonly truncated at clast margins, are present in less than 1-2% of both carbonate and non-carbonate lithic clasts in individual breccia samples. These intra-clast fractures are, nevertheless, an indication of fracturing

and any associated calcite cementation occurring prior to reworking of the lithic clasts. This is as opposed to the fractures that cross-cut the fabric of the breccia that must have formed after the material was reworked and deposited downslope as the breccia units. The thin section evaluation of potential relative timing of fractures was from 164 thin sections from the key measured sections. An additional 45 thin sections of the slope deposits had clasts too small to meaningfully evaluate intra- versus extra-clast fracturing.

Results: Diagenetic Features from Petrography

Diagenetic features are described in their most common order of occurrence, as inferred from thin section petrography. There is, however, some variation in the relative timing of events between samples.

Micritisation: Micritisation of carbonate allochem margins pre-dates all other diagenetic features. Light to dark brown micritic rims to allochems as seen under plane-polarised light microscopy are generally between 20 - 30 μm (Fig. 5 a, b and c). Micritisation is seen in almost all thin sections, but the area of micritic rims in individual thin sections is mostly <2-5%. Grain micritisation is seen in all the different facies, but generally only as trace amounts in the basinal marls, planktonic foraminifera wacke/packstones and breccia units. Trace amounts of micritisation also occur in some shallow-water grainstones and wacke/packstone units from the Central, Northern and Eastern Areas. Samples having the most common micritisation, including micritic envelopes encircling grains with rims up

to 40 μm thick, include larger benthic foraminifera wacke/packstone and coral floatstones from the Central and Eastern Areas (Fig 5 a, b and c). The CL signature of micritised rims is usually dull to non-luminescent: similar to, or slightly brighter than, the marine bioclasts they encircle.

Cavities and pore-lining cements: Pore-lining cements are uncommon in the Tonasa Formation, present in 19 out of 153 samples studied, with the additional samples not selected for this study containing almost none of these cements. Pores, or cavities that these cements line fall into two categories: (1) primary intergranular or shelter pores between bioclasts or lithic clasts that are on a mm- to cm-scale (Fig. 6), and (2) secondary dissolution cavities that cross cut strata and are on decimeter-scale (Fig. 7). Dissolution cavities are irregular in shape, have sharp, truncational margins with the host limestone and may be linked vertically by fractures and/or dissolution pipes. These dissolution cavities were found in 4 localised areas of the Tonasa Limestone Formation (Wilson et al., 2000). (1) Associated with the northernmost faulted basement high of the Barru Block (Fig. 2) in reworked shallow-water limestone clasts derived from the northern faulted margin in the late Eocene. A few metre-scale Late Eocene shallow-water carbonate outcrops that fringe the southeasterly dip-slope of the Barru Block faulted basement high also include dissolutional cavities (Wilson and Bosence, 1996). (2) Dissolutional cavities are seen in limestone clasts reworked during the Early Miocene in a basinal graben and within *in situ* shallow-water Early Miocene limestones 2 km to the west of the graben, both in the western Segeri area. (3) Four kilometres SW of the western Segeri sections in the northernmost part of the central Pangkajene area one Late Oligocene bed of peritidal algal laminites with

the overlying bed having interpreted gas escape structures are associated with reddened surfaces and irregular dissolutional cavities (Fig. 7). Late Eocene shallow carbonates in the same vicinity also contain irregular dissolutional cavities with reddened infill. (4) In the eastern area irregular dissolutional cavities are associated with erosion and tilting of strata. In the Malawa West, Ujunglamuru, Maborongnge and Bantimala measured sections Late Eocene limestone with irregular dissolutional cavities containing fine sediment are overlain by volcanics of the Camba Formation via an angular unconformity. Early Miocene shallow water carbonates at Camba have irregular dissolutional cavities of centimeter to decimeter-scale that are coated in speleothem stalagtitic and stalagmitic precipitates and containing infills of fine carbonate sediment interlaminated with layers of cave pearls (Fig. 7). The shallow-water Miocene limestones have a highly rugose upper contact with the Camba Formation at Camba and dissolution cavity infills are cut by fractures containing volcaniclastic sediment (Fig. 7). Shallow water deposits of Early Oligocene age in the Biru area bordering the western margin of the Walanae Graben have a reddened brecciated upper surface that is overlain by Late Oligocene packstones and grainstones containing planktonic foraminifera. The Bua and Birau Menge sections have irregular dissolutional cavities in Early Oligocene carbonates a few metres below an erosional and angular discordant contact with overlying Late Oligocene deposits. None of the areas with dissolution cavities can be traced for anything more than a few metres to ten metres in outcrop. In the often highly vegetated and dripstone covered upstanding karst of the Tonasa Limestone Formation it is, however, rare to be able to trace individual bed surfaces over greater extents than this. All of the irregular

dissolutional cavities occur within 5 km and more usually 1-2 km of known grabenal and horst associated faults (Wilson et al., 2000).

Included in the pore lining cements are a range of cement types that are commonly preserved as ghost textures being overprinted by later granular mosaic cement (Fig. 6a). This overprinting can render it difficult to precisely define the earlier pore lining cement phase. No pore lining cements were seen in samples from the southern Jeneponto Area. Radiaxial bladed to fibrous cements line (shelter) cavities between bioclasts or clasts in grainstone or lithoclastic facies from 4 samples associated with the platform margin in the eastern and western areas (Fig. 6b and c). Radiaxial cements have sweeping extinction patterns and crystal lengths up to 2 mm (Fig. 6c). Bladed to banded, or bladed to possible isopachous fringing cements were noted in central (1), northern (11, Fig. 6d), western (3: Fig. 6e) and eastern (2: Fig. 6a and f) area samples. These bladed and isopachous crystals fringes generally have crystal lengths less than 200 μm and occur around bioclasts in grainstone units (Fig. 6e). Longer bladed to banded crystals (up to 400 μm) fringe dissolutional cavities just in the eastern, western and northern area samples (Fig. 6d and f). Dog tooth to scalenohedral crystals are rare being present in 4 northern, 1 western and 2 eastern area samples (Fig. 6g). These dog tooth crystals are generally <200 μm and partially line dissolutional cavities (vugs to biomolds) or primary pore spaces. Micrite or crystal silts (dolomitic) may partially infill pore spaces after the pore lining cement phases (Fig. 6). Cave pearls partially infill cement lined dissolutional cavities in the eastern area (Fig. 7; after Wilson, 2000). There may be up to three phases of the

same or different pore lining cements in individual samples, some separated by micrite and/or crystal silt (Fig. 6). The CL character of pore lining cements is commonly non luminescent, or more rarely slightly bright, but towards crystal margins there may be bright and dull-luminescent zones (Fig. 6h).

Syntaxial overgrowths: Syntaxial overgrowth cements are noted in 101 of 153 thin sections, most commonly on echinoderm grains and rarely on larger benthic foraminifera. Overgrowth cements may both pre-date, but more commonly post-date, some of the mechanical grain packing and grain breakage features described directly below (Fig. 8a, b, c). On average syntaxial overgrowths comprises < 0.1% cement throughout the deposits of the Tonasa Platform with overgrowth thicknesses generally < 300 µm (Fig. 8d, e, f). Syntaxial overgrowth cements are most prevalent and thickest (up to 1 mm; Fig. 8b, c) in medium to coarse grained bioclastic planktonic foraminifera and graded bioclastic packstones from slope settings as well as in bioclast packstones and grainstones from the central Pangkajene Area. The echinoderm plates generally have a 'speckled, dusty' appearance, whereas the syntaxial cements that overgrow them are clear, to slightly turbid under plane polarised light (Fig. 8e). Cathodoluminescent imaging reveals the echinoderm grains have 'speckled' dull to non-luminescence, with up to four CL zones in the overgrowth cements. From oldest to youngest these CL cement zones are: (1) dull-, (2) non-, (3) bright-, to (4) bright to dull-luminescent (Fig. 8d-f).

Grain alignment, distortion, mechanical grain packing, grain breakage and grain suturing: Grain distortion, mechanical grain breakage and closer grain packing, the latter

including tangential and concavo-convex grain contacts, is prevalent throughout deposits of the Tonasa Platform (seen in 95% of samples studied). The degree of closer grain packing, grain breakage and sutured grain contacts is highly variable, but is most noticeable in some shallow water grainstones, larger benthic foraminifera packstones, planktonic foraminifera bioclastic packstones and breccia units (Fig. 5d, e, f). Grain distortion mostly affects micritic walled bioclasts, such as imperforate foraminifera (Fig. 5d), or marly breccia clasts. Grain breakage most commonly affects elongate grains, such as mollusc shells or flattened larger benthic foraminifera (Fig. 5e). The features described here are generally most common in the deeper Eocene and Oligocene parts of thicker sections (Figs. 3 and 4). In sections associated with deepening during fault breakthrough there is a peak in these features in deposits formed around the initial period of deepening (e.g., Rala, Figs. 3 and 4; cf. Wilson, 1999; Wilson et al., 2000).

Granular mosaic calcite: Granular mosaic calcite is present as trace to common, or more rarely abundant, amounts in 90% of samples from all areas of the Tonasa Formation, i.e., this is the most common crystal type throughout the Tonasa Formation (Figs. 5b-d, 8a-d). Granular mosaic calcite is composed of roughly equidimensional small crystals (<100-300 μm, with average size ranging from 50 to 100 μm) with irregular to subhedral crystal boundaries (*sensu* Flügel, 2004; Figs. 5b-d, 9a-d). The granular calcite may be clear crystals filling pore spaces or incorporate 'dusty' micritic patches (Fig. 9a-c), or overprint earlier cement phases (Fig. 6a). Granular mosaics may also occur in place of bioclasts as regions of clear crystals or preserving 'ghost' textures of the precursor grain (Fig. 9d and e). Near

complete replacement of samples by granular mosaic calcite preserving a range of these textures has occurred by non-ferroan and ferroan calcite in the northern, southern and eastern areas. Granular mosaic calcite is mostly dull-luminescent to non-luminescent. Although variable in their distribution, granular mosaic cements are most common in the Eocene and Oligocene deposits, commonly in thicker sections (Fig. 3 and 4).

Fracturing: Fractures here refer to through going features that cross cut more than individual grains, of which the former are grouped under mechanical grain breakage (described above). The relative timing of fractures varies, and individual samples may include multiple phases of fracturing (Figs. 9c, f and 10a, b). Fractures linking, or associated with, dissolutional cavities where fractures pre-date some cavity or fracture infill by sediment are most common in the eastern area (Fig. 9b), and more rarely occur in the northern and northern central area samples (Fig. 7). Rare samples may include multiple phases of sediment and cement infill of fractures up to 5 mm across (Fig. 6f). Other fractures not associated with cavities include sub-mm width fractures that are on a mm- to cm-scale length, commonly terminate within the sample (Figs. 9c and 10c). These fractures have irregular to diffuse margins that may merge into the groundmass. Fill of these fine scale fractures is most commonly by granular mosaic cement with crystal size commonly <100 μm (Fig. 9c). Millimetre thickness fractures and or fractures with sharp margins commonly post-date the small diffuse margined fractures and the larger-scale fractures may terminate within the thin section or be through going (Fig. 9c, f). The larger-scale, or sharp margined fractures commonly cross-cut earlier features including some cement phases. The sharp-

margined fractures are most commonly filled with blocky to equant cements with crystal sizes up 500 μm (Fig. 9f). Up to three phases of fracturing are present in samples, including 2 phases of sharp margined fractures. Some of the sharp margined fractures infilled with equant cement terminate at stylolites, but others post-date stylolitisation (Fig. 10a and b). Displacement along fractures, most commonly on a millimetre-scale, is observed from all areas except the southern Jeneponto region (Fig. 10c). Fracture development, particularly of the fine-scale fractures may be most clearly seen under cathodoluminescent images.

Fault and fracture orientations and their occurrence: A number of mainly coincident trends occur in both the large-scale near-vertical faults and smaller-scale fracture (and vein) orientation data derived from the published geological maps and field measurements (Fig. 11; after Sukamto, 1982; Sukamto & Supriatna, 1982; Wilson, 1995). A dominant NW-SE trend occurs in all areas of South Sulawesi (Fig. 11). Large-scale faults with this orientation faults mainly affect the Tonasa Limestone Formation and the lower member of the Camba Formation, but do not appear to penetrate far into the upper volcanic member of the Camba Formation. A NNW-SSE trend also affects all formations (including the upper Camba Formation) in the Walanae Depression, the eastern part of South Sulawesi and the Pleistocene/Pliocene volcanics in the southern part of South Sulawesi (Fig. 11). A possible NE-SW subsidiary fault trend also occurs in western, eastern and southern parts of South Sulawesi (Fig. 11). The fault trends affecting the Pleistocene/Pliocene volcanics in the southern part of South Sulawesi appear to be more randomly oriented. Small-scale fractures and calcite filled veins in the Tonasa Limestone Formation show predominantly the same main trends as the larger-scale faults (Fig. 11). Particularly close to major faults, small-scale fracture and veins trends are commonly

parallel, and also perpendicular to the strike direction of the main faults. In the northern area of the Tonasa Limestone Formation NW (-SE) trends predominate, with common NNW (-SSE) and NE (-SW) strike trends of the small-scale features. In the western and eastern areas the NNW (-SSE) and NE (-SW) to ENE (-WSW) trends predominate. Fracturing was less commonly recorded in the central and southern areas, and these fractures have more variable orientations when compared with other areas of the Tonasa Limestone Formation (Fig. 11).

Among the in place predominantly shallow water deposits the ratio of numbers of all fractures/veins to numbers of samples studied is consistently higher by up to tenfold in the northern, eastern and western areas of the Tonasa Limestone Formation compared with the central and southern areas (Fig. 12). Only in Eocene deposits from the central area (Lapangan Golf section) does the ratio of the number of all fractures/veins approach that from other regions. In this Eocene section the higher ratio compared with other central area sections is mainly due to straight fracturing (Fig. 12). The ratio of the number of highly irregular fractures to the number of samples studied is also consistently higher by three to eight times in the northern, eastern and western areas compared with the central and southern areas of the Tonasa Limestone Formation (Fig. 12). Sediment gravity flow deposits are just found in the northern, eastern and western areas, containing material commonly derived from faulted highs (Wilson and Bosence, 1996; Wilson, 1999; Wilson et al., 2000). In all these three areas gravity flow deposits include intra-clast, calcite-filled fractures (Fig. 12). These fractures or veins are truncated at the clast margin and occur in both lithified carbonate and non-carbonate reworked clasts. Fractures or veins that cross-cut the fabric of the lithoclastic breccias are also present in many samples from the northern, eastern and

western slope to basinal deposits (Fig. 12). There are no strong trends in ages of deposits compared with irregular and straight fractures or for intra- versus extra-clast fractures (Fig. 12).

Pore and fracture filling cements: Although granular mosaic crystals occlude some intra-, and intergranular porosity as well as some of the fine-scale fractures, this cement type is described previously. Additional crystal types that post-date and may grade from granular mosaic cements, and also fill fractures are blocky, equant, poikilotopic and rarely drusy cements (Fig. 10d-f). In less than 5% of fractures there are bladed to fibrous 'slickencrysts' that have their direction of elongation perpendicular or oblique to the fracture wall. All these commonly late stage cements are present in 40-60% of samples from all areas of the Tonasa Formation. Equant cements have equidimensional crystals up to 200 μm, and are euhedral, whereas blocky cements are coarser (up to 800 μm) and less equidimensional than the equant ones (*sensu* Flügel, 2004, Fig. 10d and e). Poikilotopic crystals are larger than 400 μm, enclose a number of allochems, and were seen in 4 western and northern area samples. An unequivocal sequential increase in crystal size towards pore centres typical of drusy cements was seen in just 4 samples from the western and northern areas (Fig. 10f). There is common gradation of pore filling cements from one type to another with: (1) drusy cements transitioning to blocky cements, (2) granular mosaic cements grading to equant or blocky cements, and (3) equant cements grading to blocky cements. Most cements are non-ferroan calcite, but in all areas except the central area ferroan calcite is

also present in up to 15% of samples. Where there are gradational changes within samples from non-ferroan to ferroan calcite the ferroan calcite as blocky cements is most commonly the final pore filling phase. There are, however, also samples in the eastern and northern areas from near the contact with the underlying siliciclastics, or adjacent igneous rocks in which ferroan granular mosaic or more rarely drusy crystals grade to non-ferroan to blocky crystals (Figs. 9b and 10f). Near complete replacement of samples by equant calcite preserving a range of these textures has occurred by non-ferroan and ferroan calcite close to some of the igneous intrusions in the northern and eastern areas (Fig. 9e). Most of the pore filling cements described in this section are dull-luminescent, but rare non- to bright luminescent zoning is seen in some blocky cements (Fig. 6h). Although variable in their distribution, equant to blocky cements are generally most common in the deeper parts of sections (Fig. 3 and 4).

Stylolites and Dissolution Seams: A continuum of 'jagged' stylolites to 'anastomosing' dissolution seams have been recognised in different areas of the Tonasa Formation (Fig. 13a). Dissolution seams are most common in samples containing more than a few percent insolubles, mostly as clays, such as deep water marls or those close to the contact with the underlying siliciclastic Malawa Formation. Stylolites are mostly bed parallel, but also occur as circum-clast stylolites in the slope breccia units. Stylolitisation and/or seam formation usually post-dates all other diagenetic features, but can be associated with, or pre-date, some of the fracturing (Fig. 10a). Any material along stylolites and dissolution seams is generally dark in plane polarised light and usually non-luminescent under cathodoluminescence (Figs. 10a,

b and 13a). As with the pore filling cements stylolites and/or dissolution seams are generally most common in the deeper parts of sections (Fig. 3 and 4).

Dolomitisation: Dolomitisation is uncommon in the Tonasa Formation, seen in 15 out of 153 samples studied, with the additional samples not selected for this study containing almost no dolomite. Dolomite occurs as: (1) clear, intergranular rhomb shaped crystals (Fig. 13c), (2) crystal silt (crystals <50 μm across; Fig. 6d), and (3) 'dusty', mimetic or fabric replacive dolomite, the later in partially or fully dolomitised samples (Fig. 13c and d). The fully dolomitised samples are restricted to the central area (3 samples), have been affected by dissolution of bioclasts, such as foraminifera, post mimetic, 'dusty' dolomite formation, then formation of dolomite cements and late blocky to poikilotopic non-ferroan calcite formation. CL images reveal non- to dull-luminescent mimetic dolomites followed by dolomite and calcite crystal growth that are mainly non- to dull-luminescent with bright zones (Fig. 13c and d). The dolomite crystals silts were seen in cavities from the eastern area previously fringed by earlier pore lining cements (Fig. 6d). Intergranular dolomite rhomb formation was seen in central, northern and eastern area grainstones, with rhombs up to 200 μm and showing some zoning with darker bands (PPL) and bright to non-luminescent zones in CL.

Results: Stable isotope analyses

Stable isotope analysis has been run on 36 samples from across the Tonasa Limestone Formation with the exception of the southern Jeneponto area. The

values of selected samples are widely scattered between 2.38‰ and –14.23‰ $\delta^{13}C$, and from –1.71‰ to –19.68‰ of $\delta^{18}O$ (Fig. 14; Table 1). Within this stable isotopic variability three groupings and one outlier are distinguished that relate to the components and their isotopic signatures (Fig. 15). The groups are: (1) a variety of components which include dolomite, blocky calcite, micrite, micritic cavity infill after radiaxial fringing cement and large benthic foraminifera that comprise the largest group (26 samples) having values of 2.38 to -0.60‰ $\delta^{13}C$ and -1.71 to -9.47‰ $\delta^{18}O$, (2) 4 samples including algal laminite and larger benthic foraminifera close to the algal laminite or the underlying siliciclastics with low negative values $\delta^{13}C$ ‰ and negative $\delta^{18}O$ ‰ values ranging between -2.04 ‰ to -3.40‰ and -6.28 to -7.60‰, respectively, and (3) 5 samples including larger benthic foraminifera, pore-filling equant cement, micritic sediment infilling dissolution cavities and blocky cement with highly negative values of -9.11 to -14.23‰ $\delta^{13}C$ and -14.20 to -19.68‰ $\delta^{18}O$. Samples from this third group all lie within 2 km of intrusive igneous stocks (with stocks exposed at the surface forming 1 to 2 km across sub-elliptical features). The outlier sample (1.79‰ $\delta^{13}C$ and -13.86‰ $\delta^{18}O$) is from a larger benthic foraminifera (Nummulites) from a localised outcrop in the eastern area surrounded by siliciclastics and close the Walanae Fault Zone and igneous intrusives.

Diagenetic Interpretations

The varied diagenetic processes and cementation phases affecting the Tonasa carbonate platform are discussed below in their most common relative order of occurrence as inferred from petrographic relationships (Fig. 15). Regionally for SE Asia, known $\delta^{18}O$ V-PDB values of Oligo-Miocene marine components and marine cements plot between -1.4 to -7.1‰ (Ali, 1995; Wilson and Evans, 2002; Madden and Wilson, 2012; 2013; Wilson et al., 2013). Some of these values fall more negatively than the global norm (Tomascik et al., 1997; Wilson, 2008). The most negative values are from palaeo-inshore areas affected by terrestrial runoff, likely reflecting lower salinities and more brackish conditions compared with the global norm (Madden and Wilson, 2013; Wilson et al., 2013). Six of the 11 sampled larger benthic foraminifera from the Tonasa Formation have $\delta^{18}O$ V-PDB values between -1.71 and -6.40‰ (and slightly positive $\delta^{13}C$ values of 0.28 and 1.96‰) that are consistent with marine values for SE Asia. Using the equation of Anderson and Arthur (1983) and at seawater temperatures of 26-30°C for modern surface waters in the Makassar Straits (Gordon, 2005; Peñaflor et al., 2009) these values from the Tonasa Formation convert to 1.4 to -4 V-SMOW. A $\delta^{18}O$ value of -6 to -4‰ V-SMOW is suggested for possible meteoric parent fluids on the basis of $\delta^{18}O$ values of meteoric precipitation in SE Asia at low elevations (Anderson and Arthur, 1983; Bowen and Wilkinson, 2002). To evaluate potential burial depths and temperatures the onset depth of stylolite and dissolution seam formation may

commonly start from 500 m is utilised (Finkel and Wilkinson, 1990; Lind, 1993; Railsback, 1993; Nicolaides and Wallace, 1997). Temperature gradients of between 21 to 28°C per kilometre have been measured in nearby subsurface wells that penetrate the Tonasa Formation (Hall, 2002b).

Micritisation: Micritisation is the first alteration process affecting most samples; since other diagenetic features cross-cut micrite envelopes and micritic rims to allochems. Micritic rim formation is inferred to be via infilling of microborings formed by endolithic organisms since micritisation generally encroaches into bioclasts within the Tonasa Formation (cf. Bathurst, 1966; Gunther, 1990; Perry, 1999). Common micritisation in packstones, floatstones and wackestones from platform-top deposits, but only trace amounts in slope and basinal deposits, is consistent with enhanced endolithic organism activity in shallow-water influenced by low to moderate energies (Fig. 1a and b; cf. Swinchatt, 1965; Budd and Perkins, 1980; Perry and Bertling, 2000; Perry and Macdonald, 2002; Perry and Hepburn, 2008). The thickest (40 μm) development of micrite rims in wacke/packstone and floatstones from shallow platform top and inner shallow platform environments in the eastern and central areas is consistent with shallow, warm waters but may also link to more nutrient-rich areas (cf. Golubic et al., 1975; Budd and Perkins, 1980; Perry, 1998, 1999; Perry and Larcombe, 2003). Constructional micritic envelope formation is also a possibility, and is often associated with seagrass facies that have locally been inferred for the Tonasa Platform (cf. Perry, 1999). The dull-luminescent to non-luminescent CL properties of the micritic rims and their similar

CL character to the bioclasts is consistent with associated marine waters and/or oxidising pore fluids.

Cavities and Pore-lining cements: Pore-lining cements are very rare in the Tonasa platform; but five early cement types are associated with platform margin and/or block faulted highs areas. Some samples including these cements are now, however, present as reworked clasts in lithoclastic slope breccias. (1) The radiaxial bladed to fibrous cements are interpreted as marine cements on the basis of their growth forms, occurrence in shelter or intergranular porosity, early pre-compactional timing and geochemistry (cf. Halley and Scholle, 1985; Flügel, 2004). Delta $\delta^{18}O$ and $\delta^{13}C$ V-PDB values of -3.6 and +2.1‰, respectively, for the one radiaxial cement sampled are consistent with the marine stable isotopic field for SE Asia. (2) The <200 µm bladed to possible isopachous fringing cements were too small to sample, but on the basis of their geometry and early timing pre-dating compaction are probably also of marine origin. These radiaxial to bladed and 'short' bladed to fringing cements are from grainstones or fringe shelter porosity in deposits close to the platform margin. Cementation is likely to be controlled by flushing of high volumes of marine waters into porous sediments along the platform margin as well as CO_2 degassing driven by high wave and tidal energy (cf. Land and Moore, 1980; Moore, 1989; Madden and Wilson, 2013). Micrite that infills some of the larger shelter pores after the pore-lining cement may have a laminated to slight peloidal character and is a feature common in other marine cavities. The rare: (3) long bladed (up to 400 µm) to banded crystals and (4) dog

tooth to scalenohedral crystals are here interpreted as mainly having a probable meteoric origin on the basis of them lining dissolutional cavities, having similar forms with known meteoric cements and in some cases being post-dated by features such as cave pearls (cf. Dreybrodt, 1988; Frisia et al., 2000). One example of dogtooth to scalenohedral cement has geochemistry consistent with SMOW values of -4.5 to -3.5 ($\delta^{18}O$ V-PDB value of -6.54‰) at surface conditions of 25-30˚C (i.e., meteoric transitional to marine parent fluids) and carbon values most consistent with a rock or marine derived signature ($\delta^{13}C$ V-PDB value of 1.98‰). (5) Micritic sediment infilling cavities is here inferred to be of either infiltered marine sediment or of karstic infill origin. Individual interpretation of micritic infills depends on: (a) whether the sediment co-occurs with dissolution or non dissolutional cavities, (b) associations with cements of marine or meteoric origins, and (c) sometimes the micrite geochemistry (for the latter see the paragraph below). The origin of the very rare dolomite crystal silts is discussed below under dolomites. The CL signature of pore lining cement with predominantly non luminescence is consistent with oxidising conditions, with some evidence for fluctuations in geochemistry and/or redox conditions of the precipitating fluids (Moore, 2001; Boggs and Krinsley, 2006).

Evidence for potential subaerial exposure and karstification of the Tonasa Limestone Formation is highly localised to faulted highs usually within 1-2 km, but rarely up to 5 km from platform margin and/or graben bounding faults, i.e., affecting less than 2% of the platform. Indicators of subaerial exposure include: (1) irregular dissolutional cavities cross-cutting strata on a decimeter-scale,

associated with, (2) in one location algal laminite and fenestral deposits, (3) speleothem stalactite and stalagmite fills, (4) banded cements, (5) cave pearl infill (6) reddened and/or brecciated surfaces, and (7) hiatal surfaces and/or angular unconformities (see also Wilson et al., 2000). Cave pearls and dog-tooth to scalenohedral cements or banded cements with speleothem geometries are distinctive of infill of karstic cavities (cf. Esteban and Klappa, 1983). The geochemical signature of these cavity infill features and the associated interlaminated micritic infill measured in this study is, however, not always distinctive of meteoric conditions. For example, although analysis of some of these features revealed negative $\delta^{13}C$ V-PDB values, 2 of the 4 analyses of this type had positive $\delta^{13}C$ V-PDB values. It may be that in regions of very limited areal extent of exposure, as is inferred here, little in the way of soil horizons may develop, and consequently there may not always be a characteristic soil-zone influenced negative carbon isotopic signature. Additionally, with the very high rates of dissolution that occur during subaerial exposure in the equatorial tropics, together with the common neomorphic replacement of early pore lining cements it is probable that a rock-derived signature (in this case of primarily marine origin) may outweigh other potential signatures (cf. Wilson, 2012). Of the localized areas with inferred subaerial exposure the timing of emergence, where constrained, is inferred to be: (1) Late Eocene – on the northern platform margin associated with the Barru Block, (2) possibly Late Eocene, but more definitely mid Oligocene and Early Miocene associated with highs surrounding the graben in the western area, and (3) around the mid Oligocene for the Birau Menge, Bua and Biru S sections and during the Early Miocene prior to the deposition of the volcaniclastics in the

Camba sections all from the eastern area (cf. Wilson et al., 2000). For other sections in the eastern area (Bantimala, Malawa West, Ujunglamuru and Maborongnge) probable karstification and tilting of strata is unconstrained to during or after the Late Eocene and before the Middle Miocene (cf. Wilson et al., 2000).

Syntaxial overgrowths: Syntaxial overgrowth cements are an early diagenetic feature because they mainly pre-date mechanical compaction but post-date some pore-lining cements. The distribution of syntaxial overgrowths is here linked to the primary distribution of echinoderm material and more open grainy sedimentary textures with higher potential for flushing by precipitating pore fluids (cf. Madden and Wilson, 2013). Inclusion-rich, turbid syntaxial overgrowths have been linked to marine-phreatic conditions, whereas clear overgrowths may form during shallow burial, with both phases occurring in the Tonasa Formation (Tucker and Wright, 1990; Flügel, 2004; Swei and Tucker, 2012). The speckled appearance of echinoderm grains in CL partly reflects micritic or cement infill within their microporous structure. The initial dull- and predominantly non-luminescent character of the early overgrowth cement is similar to the overgrown grain and consistent with precipitation from marine oxidising fluids. The succession of CL zones from non-luminescence to bright to dull in the syntaxial overgrowths is a common zonation associated with the increasingly reducing nature of pore fluids during increasing burial (Tucker and Wright, 1990; Flügel, 2004; Boggs and Krinsley, 2006).

Grain alignment, distortion, mechanical grain packing, grain breakage and grain suturing: All of these burial compactional-related features formed after both micritisation and minor early cement phases (i.e., pore lining cements and some syntaxial overgrowth cements) and therefore generally pre-date full lithification of most samples (Fig. 5d). A range of point, tangential, concavo-convex and sutured contacts likely reflect increased burial compaction relative to lithification, but may also be grain and lithology influenced (Fig. 5d, e and f; Taylor, 1950; Goldhammer, 1997; Flügel, 2004). In grainy sediments this continuum from closer grain packing to pressure solution at grain contacts may occur over burial depths of 100 m up to 700 m, but such depth ranges would likely be lower for matrix-dominated samples (Goldhammer, 1997; Flügel, 2004). Grain distortion has mostly affected grains such as micritic-walled foraminifera or marl clasts that are prone to plastic deformation (cf. Madden and Wilson, 2013). Elongate bioclasts are most prone to brittle mechanical breakage. Overall the degree of grain-related compactional features is most prevalent in lithologies that: (1) experienced little early cementation, (2) contain grains or lithologies that are prone to grain breakage, grain distortion or suturing, and/or (3) were strongly affected by burial prior to full lithification. For example, breccias and planktonic foraminifera bioclastic packstones are common in the thicker successions from the northern, eastern and to a lesser extent southern and western areas that experienced the greatest (fault-related) tectonic subsidence (Wilson, 1999; Wilson et al., 2000). These lithologies typically experienced limited early cementation and contain marly clasts or micritic matrix prone to greater differential compaction compared with more competent bioclasts or lithic clasts. The prevalence of grain-scale

compactional features in the deeper Paleogene parts of thicker sections and associated with deposits formed during fault-related deepening are together suggestive of the important roles of differential subsidence and overburden covering by subsequent carbonate sedimentation in generating early compactional features.

Granular mosaic calcite: The granular mosaic calcite is partially neomorphic to replacive in origin because it includes 'ghost' textures of earlier bioclasts or cements, or patches of micrite. Some primary calcitisation into pore space is near contiguous with neomorphism or replacement. A burial origin is inferred since granular mosaic calcite post-dates some grain compaction features, including mechanical grain breakage. Pre-dating other cementation, fracturing and compaction features (described below) a shallow burial environment of diagenesis is most likely for the granular mosaic calcite. The predominant dull-, to non-luminescent CL character of the calcite may indicate oxidising to slightly reducing pore fluids (Boggs and Krinsley, 2006), consistent with inferred shallow burial origins. Granular mosaic calcite that replaces the only known algal laminite layer from the northernmost Central area of the Tonasa Limestone has $\delta^{13}C$ V-PDB values of -2.67 and -3.40‰ indicative of soil zone process influences (cf. Hudson, 1977; Moore, 2001). The mosaic calcite must have formed very early after deposition since 'ghost' traces of the algal filaments show only minor evidence for compaction. The formation of algal laminites, their early alteration to granular mosaic calcite and $\delta^{13}C$ and $\delta^{18}O$ (-6.82 and -7.35‰ V-PDB) of the calcite are all

consistent with a meteoric influence during deposition and subsequently during near surface diagenesis for this unit. A larger benthic foraminifera sampled from 2 m below the algal laminite unit (-2.23 and -7.60‰ $\delta^{13}C$ and $\delta^{18}O$ V-PDB, respectively) and one from near the contact with the underlying siliciclastics (-2.04 and -6.28‰ $\delta^{13}C$ and $\delta^{18}O$ V-PDB, respectively) that group isotopically with the algal laminite samples are also inferred to have been influenced by meteoric fluids during near surface diagenesis. For other granular mosaic calcite that post-dates early compactional features positive $\delta^{13}C$ V-PDB values indicate a lack of soil zone processes, and that a seawater or rock-derived source of carbon with marine $\delta^{13}C$ values was inherited by the precipitating fluids (cf. Hendry et al., 1999). At shallow to moderate burial depths prior to the onset of depth of stylolite formation (around 0.5 to 1 km burial; i.e., around 35-50°C) the $\delta^{18}O$ of -5.46 and -9.47‰ V-PDB suggest parent fluids of V-SMOW predominantly between +1.3 and -3.0, i.e., most consistent with pre-cursor marine fluids. For the $\delta^{18}O$ value of -9.47‰ V-PDB in the lower part of the potential temperature range this would convert to a V-SMOW of down to -5.4 (i.e., potentially of meteoric origin). Since the granular mosaic cements with the most negative $\delta^{18}O$ values, however, are transitional to equant calcite, and also from the centre of pores, the values from the higher part of the temperature range are considered more likely converting to V-SMOW of -2.8 (i.e., more consistent with fluids of marine origin). The most

common occurrence of granular mosaic cements in the Paleogene deposits, particularly in thicker sections is likely a reflection of the influence of rates of differential subsidence and timing of overburden carbonate sedimentation in generating these shallow to moderate burial depth diagenetic phenomena (Fig. 3 and 4).

Fracturing: Multiple phases of fracturing with different origins have locally affected the Tonasa Limestone Formation since these features may cross-cut a diverse range of bioclasts and cements, and may be filled with varied cements and/or sediment fill. For the early fractures associated with cavities a karstic or marine collapse origin is inferred. The interpretation depended on whether cavities are: (1) on a decimetre-scale, irregular, dissolutional and filled with early meteoric pore fringing cements and cave sediments, or (2) predominantly shelter cavities, that lack dissolutional margins, are commonly on a centimetre-scale and are filled with early marine cements and sediment, respectively (see earlier pore-lining cements section). For the main non-cavity-associated group of fractures within the Tonasa Formation burial, unroofing and/or structural origins are inferred (see also section below on fracture orientations and evidence for their relative timing). The sub-millimetre scale irregular fractures with diffuse margins that are mainly filled by granular mosaic calcite likely formed in shallow burial depths during the lithification process (see granular mosaic cements above). Millimetre-scale aperture, sharp-margined, through going fractures post-date most lithification with at least 2 phases of these features. Through going fractures that link to stylolites filled with equant cements likely result from burial and/or tectonic compressional stresses (cf. Nelson, 1981; 2001). Other late fractures filled by equant to blocky cements may have burial, unroofing and/or tectonic structuration origins

depending on their relative timings, orientations and later cement fills (see below).

Fault and fracture orientations and evidence for their relative timing: The concordance of orientation trends in small-scale fractures with those of the large-scale faults in South Sulawesi is suggestive of structural tectonic origins for many of these features (Fig. 11). The main NW-SE trend of structures that particularly predominates in the northern area parallels that of the main platform bounding faults in this area. These northern platform bounding faults also occur along strike, and with the same trend, as the large-scale regional Adang Fault (van de Weerd and Armin, 1992; Wilson, 1999). The main northern platform bounding faults were periodically active from the Late Eocene during the deposition of the Tonasa Limestone Formation and strongly influenced sedimentation patterns (Wilson and Bosence, 1996; Wilson, 1999; Wilson et al., 2000). The NW-SE structures mostly do not penetrate into strata younger than around the Early to Middle Miocene boundary (Sukamto, 1982; Sukamto and Supriatna, 1982; Wilson, 1995). The NNW-SSE trends that prevail in the eastern and western areas parallel the trend of block faulted highs and graben that developed in these areas between the Late Eocene to Early Miocene. The NNW-SSE trending faults include those associated with the Walanae Fault Zone that bound the Walanae Graben: a major structural divide separating different tectonic regions in South Sulawesi (van Leeuwen, 1981). In the field the NNW-SSE trending structures are seen to cross-cut, and therefore in part post-date other structures, including those with a NW-SE trend (Berry and Grady, 1987; Wilson, 1995). The NNW-SSE trending faults continue to be active to the present day as evidenced by recent earthquakes along the Walanae Fault Zone (e.g. Kope

Mosque, that sat at the base of the ~300 m high fault scarp bounding the eastern part of the Walanae Depression was destroyed in an earthquake in the early part of this century). In the eastern area, faults with a northeasterly to easterly trend having dip-slip displacements with throws on the order of a few metres to tens of metres pre-date deposition of the Walanae Volcanics in the late Miocene (van Leeuwen, 1981). In the southern part of South Sulawesi faults are recorded mostly in areas close to eruptive centres of volcanoes, and locally appear to radiate from eruptive centres.

That the small-scale fractures are more common in the tectonically active northern, eastern and western areas compared with the more quiescent central and southern parts of the main platform, with many fracture trends paralleling major faults, are indications of a strong tectonic influence on fracturing. The occurrence of intra-clast fractures within shallow water lithic carbonate clasts derived from the main Tonasa platform area and reworked into slope breccia of Late Eocene to Early Miocene age are indicative of structuration during development of the Tonasa Limestone Formation, i.e., evidence for syndepositional structuration. The most common occurrence of highly irregular fractures that may have formed when deposits were semi-lithified is in the tectonically active northern, eastern and western areas, and is further suggestive of syndepositional structuration. Proximal to the major faults small scale structures both trend parallel and perpendicular to the major faults, with those at right angles to the main faults suggestive of some dilatation parallel to major fault trends. Seismic and field relationships indicate significant normal displacements along major graben and platform margin bounding faults, but transtensional (sinistral) displacements are also inferred (Grainge and Davies, 1983; Berry and Grady, 1987; Wilson, 1995).

Pore and fracture filling cements: Granular mosaic cements that infill some of the sub-millimetre fractures are discussed earlier. The very rare examples of drusy cements infilling pore space may form in meteoric (or marine) phreatic to shallow burial settings, but were too small to sample for geochemical analysis. The majority of the equant to blocky cements are interpreted as shallow to deeper burial features on the basis of: (1) most being late phases of pore filling cements, (2) post-dating early compaction features, but pre-dating later compactional stylolites or dissolution seams and (3) their geochemistry. The dull-luminescent character of most of these cements is also consistent with precipitation under reducing conditions in moderate to deeper burial depths. Predominantly positive $\delta^{13}C$ V-PDB between -0.3 and +2.38‰ are consistent with precipitating fluids mainly isolated from those influenced by soil zone processes. Negative values of $\delta^{18}O$ V-PDB between -4.0 and -9.5‰ would equate to V-SMOW values of +2.0 to -5.5 at moderate to shallow burial temperatures of 35-55°C (Fig. 14; Hudson, 1977; Anderson and Arthur, 1983). Most of the blocky to equant cements are consistent with precipitation from fluids with a rock-derived and/or precursor marine fluid origin. A meteoric origin is also possible for some of the late fracture filling cements with strongly negative $\delta^{18}O$ V-PDB values, with the possibility of such a signature being linked to cementation along fractures during unroofing and present day sub-aerial exposure. The development of slickencrysts in some fracture filling cements indicates active deformation during growth of the crystals. A recrystalised larger benthic foraminifera grainstone from an isolated exposure

adjacent to the major Walanae Fault Zone has highly negative -13.9‰ $\delta^{18}O$ V-PDB (1.8‰ $\delta^{13}C$ V-PDB) perhaps due to hydrothermal activity (cf. Pichler and Dix, 1996), or ?unusual fluid chemistries, along the fault zone. A separate group of 5 samples including 2 equant cements having highly negative $\delta^{18}O$ V-PDB (-14.2 to -19.7‰) and also highly negative $\delta^{13}C$ V-PDB values (-9.11 to -14.2‰) are suggestive of both high temperatures and a possible methanogenic source of carbon. All of these last 5 samples are from close to contacts with the overlying volcaniclastics or igneous intrusions and metasomatising fluids are possibly associated with the isotopic signature (cf. Pichler and Dix, 1996). The most common occurrence of pore lining cements in the deeper parts of sections attests to the importance of overburden sedimentation in influencing late burial features.

Stylolites and Dissolution Seams: These chemical compaction features post-date almost all other diagenetic feature on the basis of cross-cutting relationships, with the exception of some fractures and their cement infills. These features form in moderate to deep burial environments with an onset depth commonly starting around 500 m (Railsback, 1993; Nicolaides and Wallace, 1997), or may form as a result of tectonic stresses (Bathurst, 1987). In the Tonasa Limestone the bed parallel examples are linked to burial compaction. The prevalence of stylolites and seams in northern, southern and some eastern sections correlates with where depositional thicknesses of the carbonate commonly exceed 1 km, and are subsequently covered in thick volcaniclastic piles. A continuum from dissolution seams to stylolites in clayey limestones to near pure carbonate lithologies,

respectively, has been noted in a range of studies (Bathurst, 1987; 1990; Railsback, 1993; Nicolaides and Wallace, 1997). In depositional units that experience little early cementation, such as the slope breccias, grain contacts between clasts during increasing burial have developed into circum-clast stylolites (cf. Madden and Wilson, 2013). As with the pore lining cements the more common occurrence of seams and/or stylolites in the deeper parts of sections attests to the importance of overburden sedimentation in influencing late burial features.

Dolomitisation: The very rare dolomite seen in the Tonasa Limestone may have multiple origins, on the basis of very different occurrences. Given the complexity of potential dolomitising mechanisms and paucity of data on these dolomites only a preliminary evaluation is outlined here (cf. Warren, 2000; Carnell and Wilson, 2004; Machel, 2004). Very rare, highly localised dolomite silts infilling dissolutional cavities of karstic origin, as occur in the eastern area, have been linked in Sulawesi and elsewhere to formation in vadose meteoric environments (Fig. 14a, b; cf. Mayall and Cox, 1988; Flügel, 2004). Seawater, however, is a key source of Mg, and particularly for some of the rare dolomite silts in shelter porosity after radiaxial cement, marine fluids are the more likely dolomitizing agent (cf. Warren, 2000; Machel, 2004). Replacive dolomitisation in the fully dolomitised samples from the central area predates the onset of stylolite formation and with $\delta^{18}O$ V-PDB values of -2.7 to -5.3‰ using the equation of Land (1983) these would convert to SMOW values of 0.4 to -5.2 (i.e. predominantly of marine parental fluid origins but potentially also of meteoric fluid origins; cf. Warren, 2000; Machel, 2004). A

change from dull-luminescent replacive dolomite to non-luminescent dolomite cements with bright zones would be consistent with a generally trend from oxidising to reducing conditions during burial with some fluctuations in geochemistry and/or redox state of dolomitised fluids (Fig. 15). The rare intergranular dolomite cements in the grainstones may also have a similar burial signature. The source of Mg for the intergranular and fully replacive dolomites may be seawater, although given that less than 1% of the platform is dolomitized there must be a local driver for the dolomitisation seen. Other potential sources of Mg are from clays in the nearby siliciclastics or perhaps more likely volcaniclastics since most partially dolomitized samples contain admixed volcaniclastics or are close to the contact with the volcaniclastics or to igneous intrusives (rich in Mg containing minerals such as biotite and locally olivine). Igneous intrusives may have provided a thermal driver for increased throughput of dolomitising fluids. This evaluation of potential dolomitising mechanisms is, however, highly speculative without further additional investigation.

Discussion

Summary of diagenetic features, their variability and controlling influences:

Petrographic and geochemical studies reveal that three main phases of diagenesis have affected most areas of the Eocene to Miocene Tonasa Formation prior to recent uplift and exposure (Figs. 15 and 16). The general relative order of these main diagenetic phases is: (1) surface or very near surface predominantly marine alteration, and highly localised meteoric diagenesis, (2) pervasive shallow to moderate burial grain-scale compaction and cementation/recrystallisation, and (3) common fracturing and deeper burial chemical compaction and cementation.

Marine phreatic, with minor meteoric effects, through to progressively deeper burial is therefore recorded in the diagenetic features of the Tonasa Platform. As discussed below these features and their variability, or paucity thereof, predominantly link to the nature of the platform deposits, their tectonic, climatic and oceanographic context, together with the location of faulted highs, basin history and differential subsidence. Many of these same factors strongly influenced the deposition and sedimentary development of the Tonasa Platform (Wilson and Bosence, 1996; Wilson, 1999; 2000; Wilson et al., 2000). This paragenetic sequence affecting the Tonasa Limestone is similar to that from a number of Eocene to Miocene platforms in the area (Fig. 15; e.g., Berai (Saller and Vijaya, 2002), and Kedango (Wilson et al., 2012; Madden and Wilson, 2013)). These other Tertiary platforms from the neighbouring island of Borneo also show limited early (marine or meteoric) diagenesis together with prevalent neomorphism, compaction and cementation linked to shallow to deeper burial diagenesis (Saller and Vijaya, 2002; Madden and Wilson, 2013). The diagenesis of the Tonasa Limestone and other similar platforms differs markedly, however, from many Neogene systems in the region that may comprise reservoirs in the subsurface (Epting, 1980; Fulthorpe and Schlanger, 1989; Grotsch and Mercadier, 1999; Vahrenkamp et al., 2004). These Neogene reservoirs with porosities of up to 10-40% commonly have a layered development due to repeated subaerial exposure and leaching in the vadose zone, pervasive phreatic cementation, with early fabrics overprinted but commonly not masked by later diagenesis (Epting 1980; Dunn et al. 1992; Zampetti et al. 2003; Vahrenkamp et al., 2004; Wilson, 2012).

Early marine and meteoric diagenesis: the role of climate, tectonic highs, oceanography and the nature of platform deposits:

Although early grain micritisation occurs in most samples its prevalence in shallow-water packstones and floatstones is consistent with enhanced activity of endolithic microborers in shallow sunlit water from the platform top where wave or current activity was not a hindrance, as is inferred for much of the Tonasa Platform (Wilson et al., 2000; cf. Bathurst, 1966; Gunther, 1990). The presence of nutrients and/or seagrass facies as is common in the equatorial tropics and is locally inferred for the Tonasa platform may also promote destructive or constructive micrite envelope formation (cf. Perry, 1999; Wilson, 2012).

Pore lining cements and subsequent cavity infill fall into two categories: of marine or probable karstic origin, with all of the uncommon occurrences associated with the platform margin, faulted highs, grainstone or slope lithoclastic facies. The occurrence of marine cements in platform margin settings, many associated with probable steep-margined upstanding faulted highs is consistent with high volumes of seawater flushed through margin deposits (cf. Land and Moore, 1980; Moore, 1989; Madden and Wilson, 2013). The globally important Indonesian Throughflow, an oceanic current linking Pacific and Indian Ocean waters, has been actively flowing north to south through the Makassar Straits region since at least the Oligocene (Kuhnt et al., 2004; Gordon, 2005). The predominant occurrence of marine pore-lining cements in more northerly northern, western and eastern platform margins areas for the Tonasa Limestone, but lack of any such features from the southern margin is a probable reflection of this oceanic throughflow pathway. The comparative lack of marine cements away from the more northerly margins is perhaps due to lower than normal marine

salinities common in SE Asia and associated reduced aragonite saturation linked to regionally high runoff and the equatorial setting (Wilson, 2002; 2012; Gordon, 2005). This is despite a moderate to high energy E-W trending seaway inferred for the main N-S trending Tonasa Platform area (Wilson and Bosence, 1997; Wilson et al., 2000). This paucity of marine precipitates and/or cementation is in marked contrast to other isolated platforms in more arid tropical regions (cf. Wilson, 2002; 2012). Turks-Caicos is one such platform from the more arid tropics that also has a marked E-W cross platform seaway, but this is a region of prevalent ooid formation, an allochem not found in the Tonasa Platform (Wanless and Dravis, 1989; Jones and Desroches, 1992).

Dissolutional cavities with speleothem, long bladed to banded, and scalenohedral to dogtooth cements of inferred karstic origin are restricted to northern, eastern and western areas from faulted highs (or reworked thereof). Tilting of rotated fault blocks and uplift of block faulted highs are considered instrumental in the development of these highly localised karstic features (Wilson and Bosence, 1997; Wilson, 2000; Wilson et al., 2000). On different block faulted highs the timing of localised karstification can be pinned down to: (1) during the Upper Eocene, (2) around the middle Oligocene, or (3) towards the end of the Early Miocene and just prior to volcaniclastics of the Camba Formation covering the platform (Wilson and Bosence, 1996; Wilson, 1999; 2000; Wilson et al., 2000). For other sections where there is a long hiatus, karstification may have occurred between the late Eocene and Early Miocene, and perhaps even repeatedly, although the multiple karstification events are not possible to constrain (Wilson et al., 2000). The late Eocene phase is linked to fault breakthrough of earlier reactivated basement structures and associated uplift of footwall highs (Wilson,

1999). The Early Miocene phase is linked to renewed faulting associated with the early stages of volcanism (Wilson, 2000; Wilson et al., 2000). Although around the middle Oligocene is a time of some regional structuration, sub-aerial exposure of highs may also be linked to a major eustatic sea level fall at this time (Saller et al., 1992; 1993; Wilson et al., 2000). Although much of the Tonasa Platform is aggradational remaining in photic depths throughout Eocene to Miocene deposition it is perhaps surprising that only extremely localised subaerial exposure is inferred for the major middle Oligocene eustatic fall (of around 50 m; Haq et al., 1987). Possible reasons for this general dearth of evidence for subaerial exposure outside faulted highs are: (1) relatively slow production rates of the larger benthic foraminiferal dominated facies limiting platform building potential (0.2-0.3 m kyr^{-1} accumulation rates; Wilson et al., 2000), (2) the mobile nature of much of the platform deposits with possible truncation of sediment affected by shallow water or current activity, as well as (3) tectonic subsidence (Wilson, 1999; Wilson et al., 2000). The preponderance of mobile deposits over framework building coral-rich deposits has been linked to the platform forming in a region of high rainfall and oceanic throughflow. In settings such as this, with a tendency towards mesotrophy low-light level oligophotic biota, including some larger benthic foraminifera and coralline algae, may be promoted (Wilson and Vecsei, 2005).

These same reasons, outlined directly above, may also be influential in the limited and highly localised occurrence of inferred subaerial exposure occurring generally within 1-2 km (rarely up to 5 km) of faulted margins and affecting less than 2% of the Tonasa platform area. Faulted highs on other syntectonic carbonate platforms are also associated with karstification (Rosales et al, 1994; Rosales, 1999; Cross and Bosence, 2008). Cretaceous

platforms from Spain show karstification generally within 1-2 km (and up to 5-6 km) of faults bounding the footwall highs: i.e., similar to the Tonasa Platform (cf. Rosales et al., 1994). On these Spanish examples, however, associated with smaller-scale fault block development trending perpendicular to the rifting direction, between 10-60% of the platform area was affected by exposure during seven phases of repeated exposure over around 8 million years (Rosales et al., 1994). The eastern area of the Tonasa Limestone has fault block development on a scale most similar to the Spanish platforms but is thought to have experienced three potential phases of exposure over around 30 million years, each affecting less than 10% of the eastern platform area (Wilson et al., 2000). Extension in the eastern area probably roughly parallels the main extensional direction in the backarc basin associated with the Makassar Straits on whose eastern flank the Tonasa Platform developed (Moss and Chambers, 1999; Wilson et al., 2000). Faulting in the eastern area, however, mainly occurred from the mid Oligocene onwards and may be linked more to structuration on the Walanae Fault Zone (Leeuwen, 1981; Wilson et al., 2000). Across rift basins, it may be during the early synrift or on rift margin flanks that subaerial exposure of carbonates on faulted highs predominantly occurs (Rosales et al., 1994; Dorobek, 2008). I.e., subaerial exposure is not always a feature of syntectonic platforms, particularly those that formed in basin centres or after initial rifting. The Tonasa Limestone Formation developed as part of a transgressive succession slightly postdating initial back-arc basin development and on amalgamated, highly varied, intersliced basement terranes (Berry and Grady, 1987; Wakita et al., 1996). Although formed on the basin margin flanks the extensional direction of the main N-S trending tilt-block platform is oblique to that of the backarc area as a whole (Wilson, 1995; Wilson et al., 2000). Regional subsidence in South Sulawesi during the deposition of the Tonasa Limestone, based on stratal thickness data was up to 20-40 m/Ma,

with higher subsidence in the adjacent Makassar Straits (Cloke et al., 1999b; Wilson et al., 2000). Inferred very limited subaerial exposure of the Tonasa Limestone Formation is likely to have been affected by: (1) developing over an area not of "typical" continental crust, (2) accumulating in an area with extension oblique to the main regional rift direction, and (3) forming on a basin margin generally undergoing subsidence rather than flank margin uplift.

Mid-stage shallow to moderate burial depth diagenesis: the role of climate, tectonic highs, the nature of platform deposits and tectonic subsidence:

Syntaxial overgrowths, grain-scale compaction and granular mosaic cement all attest to the onset of burial diagenesis on predominantly unlithified deposits as they start to lithify. Aragonitic components had generally not been dissolved prior to the onset of burial diagenesis. The petrographic and geochemical evidence points towards marine, or marine-derived fluid being the main agent during mid-stage shallow to moderate depth burial diagenesis. The prevalence of this mid-stage diagenesis throughout most deposits of the Tonasa Formation is linked to the paucity of earlier marine or meteoric cementation (and/or dissolution) affecting the platform. As noted earlier this scarcity of early cements is due to the: (1) humid climatic setting and lower than global-norm marine salinity, (2) relatively slow production rates of the foraminiferal-dominated deposits and their mobile nature hindering the potential to build directly to sealevel. Local variability in grain types (e.g., echinoderms and imperforate foraminifera) and sediment textures (e.g., more grainy textures and breccias) that link to environmental variability influence the degree of mid-stage diagenesis effects across the platform. Localised meteoric diagenesis is limited to areas of faulted high, including the algal laminites from the Tonasa-II section or to deposits within a few

metres of the underlying siliciclastics. Outside the areas of the faulted highs, shallow water platform carbonates and shallow to deeper water successions reach thicknesses of 600 and 1100 m, respectively. Rates of tectonic subsidence and the timing of overburden carbonate sedimentation are inferred to have been influential in the abundance of mid-stage diagenetic features that link to the onset and progressive burial of the carbonates. Differential subsidence, both prior to and following fault breakthrough, controlled regional variations in subsidence, influencing the localised variability in degree of shallow to moderate burial depth diagenetic affects (cf. Wilson, 1999; Wilson et al., 2000).

Fault, fracture and vein distributions, their orientations and relative timing: the key impact of tectonics:

Although the Tonasa Limestone is one is the best documented examples of a syntectonic carbonate system from its sedimentary record (Wilson and Bosence, 1996; Wilson, 1999; 2000; Wilson et al., 2000), it is arguably just in the fault, fracture and vein data that the syntectonic nature of the platform is only really strongly manifest from a diagenetic perspective. The correspondence of: (1) higher occurrences of numbers of fractures, (2) more highly irregular fractures, and (3) fractures and veins within clasts of lithoclastic slope breccias all in areas of large-scale faulting active during the deposition of the Tonasa Limestone as compared with more tectonically quiescent platform areas are, collectively, direct indicators of diagenesis coeval with tectonism. There is scope for applying analysis of this type to fracture datasets from other syntectonic platforms to more fully evaluate syntectonic diagenesis. The strong concordance of fracture and vein orientation data with larger-scale fault orientation data including faults known to be active

during the deposition of the Tonasa Limestone Formation is consistent with a link between synsedimentary faulting and small-scale fracturing. The predominant NW-SE and NNW-SSE trends, together with subsidiary trends of NE-SW to ENE-WSW either parallel platform margin and/or graben bounding faults, or are interpreted dilatational features perpendicular to the major faults. The predominant fault and fracture trends within South Sulawesi mirror those from the broader backarc basin region that encompasses West Sulawesi, the Makassar Straits and western Borneo. The major regional structures include the Adang Fault, Walanae Fault Zone and faults perpendicular to the predominant extensional direction in the backarc area. Regionally some of these larger-scale structures may involve reactivation of earlier basement fabrics, and including the ones linked with the Tonasa Limestone Formation, are associated with syntectonic sedimentation during the Tertiary (van de Weerd and Armin, 1992; Wilson and Bosence, 1996; Moss et al., 1997; Moss and Chambers, 1999; Wilson et al., 2012). The potential timing of fault movement inferred to have affected the Tonasa Limestone Formation in: (1) the Late Eocene, (2) possibly the mid Oligocene, and (3) during the Early Miocene is from the timing of highly localised subaerial exposure of footwall highs, but also in the record in the slope lithoclastic breccias, as well as stratal wedging and thickening (Wilson and Bosence, 1996; Wilson, 1999; 2000; Wilson et al., 2000). Regionally, although basin initiation began earlier, rifting was widespread by the Late Eocene, with some structuration inferred in the mid Oligocene, and then again in the Early to Middle Miocene (Van de Weerd et al., 1987; Letouzey et al., 1990; Bransden and Matthews, 1992; van de Weerd and Armin, 1992; Saller et al., 1992).

The different phases of fracturing affecting individual samples may have multiple origins on the basis of their petrography and geochemistry including: early collapse or karst-

-related, burial-associated, tectonic-induced, or uplift-related. More systematic study of the fracturing, a tie between their orientations, relative timing data and geochemistry of any cements or sediment infills that was beyond the scope of this study is an avenue for further unraveling the histories of any syntectonic diagenesis and fracturing (cf. Guidry et al., 2007; Breesch et al., 2009; Warrlich et al., 2010; Budd et al., 2013). A study of the very highly localised and enigmatic dolomitisation is also not pursued here, but may be an avenue for further potential research (cf. Carnell and Wilson, 2004).

Late-stage predominantly moderate to deeper burial depth diagenesis: the role of tectonics, basin evolution, climate, tectonic highs, oceanography and the nature of platform deposits: Most of the equant and blocky cements together with the dissolution seams and stylolites indicate that the platform was progressively affected by moderate to deeper depth burial diagenesis. As with mid-stage shallower burial diagenetic phases those associated with later burial diagenesis are commonly most pervasive in areas of greatest subsidence (e.g., the faulted graben areas) and/or where deposits had little early cementation. This predominance of burial diagenetic features dominating in large-scale Tertiary platforms is common to other SE Asian systems (Saller et al., 1992; 1993; Saller and Vijaya, 2002; Wilson et al., 1999; Wilson, 2012; Madden and Wilson, 2013). Localised evidence for early meteoric diagenesis in these other SE Asian platforms (e.g. Berai, Kedango, Kerendan, Melinau) is limited to faulted highs and/or areas with more abundant framework builders (Adams, 1965; Saller et al., 1992; 1993; Saller and Vijaya, 2002; Wilson, 2012; Madden and Wilson, 2013). The pronounced middle Oligocene eustatic sealevel fall (Haq et al., 1987) is generally only manifest on faulted and/or bathymetric highs on the platforms (Saller et al., 1992; 1993). The dominance of

larger foraminiferal (and algal) deposits, their mobile nature and limited upbuilding potential have all contributed to the prevalence of burial features and paucity of earlier non-burial linked cements in Paleogene equatorial platforms (cf. Wilson, 2002; 2008; 2012). Overall, with the exception of the fracture development, it is, if anything, a regional signature similar to other long-lived Tertiary carbonate platforms in SE Asia that shines through in the diagenetic development of the Tonasa Limestone Formation as opposed to an overriding syntectonic diagenetic signature.

Conclusions

Diagenesis of the Eocene to Early Miocene syntectonic Tonasa carbonate platform is dominated by alteration in shallow to deeper burial depths. Burial diagenesis is evidenced by mechanical and chemical compaction, as well as a range of cements including granular mosaic, blocky and equant calcite. Earlier diagenetic features include common marine phreatic micritisation of allochems. Rare, localised evidence for meteoric diagenesis is predominantly from faulted highs. These diagenetic features in the Tonasa Limestone are similar to those from other SE Asian long-lived Tertiary carbonate platforms. The Tonasa Limestone Formation is one of the best documented syntectonic platforms from a sedimentary perspective (Wilson and Bosence, 1996; Wilson, 1999; 2000; Wilson et al., 2000). On the diagenetic side, with the exception of the fracture development, it is, however, a regional rather than strong syntectonic signature that predominates. Underlying tectonic reasons, in addition to those of non-tectonic origin listed below, are inferred to be influential in the more regional

diagenetic signature predominating. (1) The platform although developing on the flanks of an extensional basin, accumulated in a backarc setting on amalgamated basement of highly varied origins. In this setting the platform would have been potentially less prone to uplift than "typical" rheologically-strong continental crust. (2) The orientation of significant synsedimentary faulting commonly influenced by earlier basement structures, was not always perpendicular to the main extensional direction in the broader basin. (3) The Tonasa Carbonate Platform formed in an extensive basinal region generally undergoing subsidence, post-dating rift basin initiation.

Tectonic uplift of faulted highs, perhaps with the overprint of eustatic sea level fall controlled highly localised karstification and meteoric diagenesis. The orientation and relative timing datasets of faulting, fracturing and calcite veining is the strongest manifestation of diagenesis coeval with tectonism in the Tonasa Limestone Formation. Orientations of both small-scale and platform bounding/ segmenting structures together with the timing of faulting are consistent with those from the broader basin, hinting at a strong regional tectonic influence. Tectonic subsidence, including fault related differential subsidence, was a key influence on the degree of burial diagenesis impacting different areas of the platform. The location of bathymetrically upstanding faulted highs together with major oceanic current systems resulted in localised marine cementation along the platform margin. The general paucity of early marine or meteoric cements is attributed to: (1) the predominance of non-framework building larger foraminifera and/or algae that have limited production rates, are prone to remobilisation, and hence limited potential to build to sea level, (2) lower than global norm marine salinities, and (3) deposition in a tectonically subsiding area. The: (1) dearth of early cementation,

(2) grain associations common in mainly Paleogene carbonate platforms from SE Asia, and (3) the equatorial climate resulting in high freshwater runoff have together contributed to the predominance of burial diagenetic impacts on carbonate platforms from tectonically subsiding regions. It is hoped that studies such as this will further contribute to understanding diagenetic alteration of syntectonic carbonate platforms, and those from equatorial regions.

Acknowledgements

This research forms a part of Hamed Arosi's PhD studies, supervised by Moyra Wilson, at Curtin University. Hamed received a PhD scholarship from the Libyan Higher Education Ministry. BP Exploration, UK and the SE Asia Research Group, London University provided the funding and logistical support for the fieldwork in Sulawesi, undertaken by Moyra as part of her PhD studies. Tony Barber, Dan Bosence, Diane Cameron, Darwis Falah, Robert Hall and Alexander Limbong are all thanked for their help in the original primarily sedimentological study of the Tonasa Formation. In Indonesia, GRDC, Bandung, Kanwil, South Sulawesi, BP offices in Jakarta and Ujung Pandang, LIPI and many people in Sulawesi all provided technical and practical support. Dr. Ted Finch and Prof. Fred Banner (deceased), both at University College London, and Dr. Toine Wonders, Consultant, UK (deceased), are thanked for their detailed biostratigraphic work. Neil Holloway at Royal Holloway, and Moyra (under the tutelage of Neil), made the thin sections. Cathodoluminescent analysis was run with the help of Francis Witkowski at Royal Holloway, London University. Stable isotope analyses were run in collaboration with Tony Fallick and Terry Donnelly at SUERC, East Kilbride, UK. We thank Robert

Madden and an anonymous reviewer, together with editor Brian Jones, for their constructive comments focusing us to improve the manuscript. This is for Fatima, Khadeeja and Siddeeg, and their futures.

References

Adams, C.G., 1965. The foraminifera and stratigraphy of the Melinau Limestone, Sarawak, and its importance in Tertiary correlation. Quarterly Journal of the Geological Society, London 121, 283-338.

Adams, C.G., 1970. A reconsideration of the East Indian Letter Classification of the Tertiary. British Museum of (Natural History), Geology 19, 87–137.

Ali, M., 1995. Carbonate cement stratigraphy and timing of diagenesis in a Miocene mixed carbonate-clastic sequence, offshore Sabah, Malaysia - constraints from cathodoluminescence, geochemistry and isotope studies. Sedimentary Geology 99, 191-214.

Anderson, T.F., Arthur, M.A., 1983. Stable isotopes of oxygen and carbon and their application to sedimentologic and paleoenvironmental problems. In: Arthur, M.A., Anderson, T.F., Kaplan, I.R., Veizer, J., Land, L.S., (Eds.), Stable Isotopes in Sedimentary Geology, SEPM Short Course No. 10, 1-1 - 1-151.

Bachtel, S.L., Kissling, R.D., Martono, D., Rahardjanto, S.P., Dunn, P.A., MacDonald, B.A., 2004, Seismic stratigraphic evolution of the Miocene– Pliocene Segitiga Platform, East Natuna Sea, Indonesia: the origin, growth, and demise of an isolated carbonate platform, in Eberli, G.P., Masafero, J.L., Sarg, J.F., eds., Seismic Imaging of

Carbonate Reservoirs and Systems: American Association of Petroleum Geologists, Memoir 81, pp. 291–308.

Bathurst, R.G.C., 1966. Boring algae, micrite envelopes and lithification of molluscan biosparites. Journal of Geology 5, 15–32.

Bathurst, R.G.C. 1987. Diagenetically Enhanced Bedding in Argillaceous Platform Limestones: Stratified Cementation and Selective Compaction. Sedimentology 34, 749–778.

Bathurst, R. G. C. 1990. Thoughts on the growth of stratiform stylolites in buried limestones. Sediments and Environmental Geochemistry, 3–15.

Berry, R.F., Grady, A.E. 1987. Mesoscopic structures produced by Plio-Pleistocene wrench faulting in South Sulawesi, Indonesia. *Journal of Structural Geology*, **9**, 563-571.

Boggs, S., Krinsley, D., 2006. Application of cathodoluminescence imaging to the study of sedimentary rocks. Cambridge University Press, New York. (165 pp).

Bowen, G.J., Wilkinson, B., 2002. Spatial distribution of $\delta^{18}O$ in meteoric precipitation. Geology 30, 315-318.

Breesch, L., Swennen, R., Vincent, B. 2009. Fluid flow reconstruction in hanging and footwall carbonates: Compartmentalization by Cenozoic reverse faulting in the Northern Oman Mountains (UAE). Marine and Petroleum Geology 26, 113–128.

Budd, D.A., Perkins, R.D., 1980. Bathymetric zonation and paleoecological significance of microborings in Puerto Rican shelf and slope sediments. Journal of Sedimentary Petrology 50, 881–904.

Budd, D.A., Frost, E.L., Huntington, K.W., Allward, P.F. 2013. Syndepositional deformation features in high-relief carbonate platforms: long lived conduits for diagenetic fluids. Journal of Sedimentary Research 82, 12-36.

Burchette, T.P., 1988, Tectonic control on carbonate platform facies distribution and sequence development: Miocene, Gulf of Suez. Sedimentary Geology 59, 179-204.

Carnell, A.J.H., Wilson, M.E.J., 2004. Dolomites in Southeast Asia - varied origins and implications for hydrocarbon exploration. In: Braithwaite, C.J.R., Rizzi, G. Darke, G. (eds.). The geometry and petrogenesis of dolomite hydrocarbon reservoirs. Geological Society of London Special Publication 235, pp. 255-300.

Cloke, I.R., Moss, S.J., Craig, J., 1999a. Structural controls on the evolution of the Kutai Basin, East Kalimantan. Journal of Asian Earth Science 17, 137–156.

Cloke, I.R., Milsom, J., Blundell, D.J.B., 1999b. Implications of gravity data from East Kalimantan and the Makassar Straits: a solution to the origin of the Makassar Straits?. Journal of Asian Earth Science 17, 61-78.

Cross, N.E. Bosence, D.W.J. 2008 Tectono–sedimentary models for rift basin carbonate sedimentation. *In:* Lukasik, J., Simo, J.A. (eds). Controls on Carbonate Platform and Reef Development. SEPM Special Publication 89, 83-105.

Daly, M.C., Cooper, M.A., Wilson, I., Smith, D.G., Hooper, B.G.D., 1991. Cenozoic plate tectonics and basin evolution in Indonesia. Marine and Petroleum Geology 8(1), 2-21.

Davies, P.J., Symonds, P.A., Feary, D.A., Pigram, C.J., 1989, The evolution of the carbonate platforms of northwestern Australia, *in* Crevello, P.D., Wilson, J.L., Sarg, J.F., Read, J.F. (eds.) Controls on Carbonate Platform and Basin Development, SEPM, Special Publication 44, p. 233-258.

Dickson, J.A.D., 1965. A modified staining technique for carbonates in thin section. Nature 205, 587.

Dickson, J.A.D., 1966. Carbonate identification and genesis as revealed by staining. Journal of Sedimentary Petrology 36, 491-505.

Dorobek, S., 1995, Synorogenic carbonate platforms and reefs in foreland basins: controls on stratigraphic evolution and platform/reef morphology. *in* Dorobek, S., and Ross, G.M. (eds.) Stratigraphic Evolution of Foreland Basins. SEPM, Special Publication 52, 127-147.

Dorobek, S.L. 2008a Tectonic and depositional controls on syn-rift carbonate platform sedimentation. *In:* Lukasik, J., Simo, J.A. (eds.) Controls on Carbonate Platform and Reef Development, SEPM Special Publication 89, 57-81.

Dorobek, S.L., 2008b, Carbonate platform facies in volcanic-arc settings: Characteristics and controls on deposition and stratigraphic development, *in* Draut, A.E., Clift, P.D., Scholl, D.W. (eds.) Formation and Applications of the Sedimentary Record in Arc Collision Zones. Geological Society of America, Special Paper 436, 55-90.

Dreybrodt, W. 1988. Processes in karst systems - physics, chemistry, geology. New York, Springer. Springer Series in Physical Environments 4, 288 pp.

Dunham, R.J., 1962. Classification of carbonate rocks according to depositional texture. In*:* Ham, W.E. (Ed.), Classification of carbonate rocks. American Association of Petroleum Geologists, Memoir 1, 108-121.

Dunn, P.A., Kozar, M.G., and Budiyono, 1996. Application of geosciences technology in a geologic study of the Natuna gas field, Natuna Sea, offshore Indonesia: 25thIndonesian Petroleum Association, Annual Convention, Proceedings, 117-130.

Epting, M., 1980. Sedimentology of Miocene carbonate buildups, central Luconia, offshore Sarawak: Bulletin of the Geological Society of Malaysia, 12, 17-30.

Elburg, M.A., Foden, J., 1999. Geochemical response to varying tectonic settings: An example from southern Sulawesi (Indonesia). Geochimica et Cosmochimica Acta 63, 1155–1172.

Elburg, M.A., van Leeuwen, T.M., Foden, J., Muhardjono, 2003. Spatial and temporal isotopic domains of contrasting igneous suites in Western and Northern Sulawesi, Indonesia. Chemical Geology 199, 243– 276.

Embry, A.F., Klovan, J.E. 1971. A late Devonian reef tract on northeastern Banks Island, Northwest Territories. Canadian Petroleum Geologist, Bulletin 19, 730-781.

Epting, M., 1980. Sedimentology of Miocene carbonate buildups, central Luconia, offshore Sarawak. Bulletin of the Geological Society of Malaysia 12, 17-30.

Esteban, M., Klappa, C.F. 1983. Subaerial exposure. In: Scholle, P.A., Bebout, D.G. and Moore, C.H. *(eds.),* Carbonate Depositional Environments, American Association of Petroleum Geologists, Memoir 33, 1-55.

Finkel, E. A., Wilkinson, B. H. 1990. Stylolitization as a Source of Cement in Mississippian Salem Limestone, West-Central Indiana (1). American Association of Petroleum Geologists, Bulletin, 74(2), 174-186.

Flügel, E., 2004. Microfacies of carbonate rocks, Springer, Berlin Heidelberg New York. 976 pp.

Frisia, S., Borsato, A., Fairchild, I.J., McDermott, F. 2000. Calcite fabrics, growth mechanisms, and environments of formation in speleothems from the Italian Alps and southwestern Ireland. Journal of Sedimentary Research, A70, 1183-1196.

Fulthorpe, C.S., Schlanger, S.O., 1989. Paleo-Oceanographic and tectonic settings of Early Miocene reefs and associated carbonates of offshore Southeast-Asia. American Association of Petroleum Geologists, Bulletin 73, 729-756.

Gawthorpe, R.L., Fraser, A.J., Collier, R.E.L., 1994, Sequence stratigraphy in active extensional basins: implications for the interpretation of ancient basin-fills. Marine and Petroleum Geology 11, 642-658.

Golubic, S., Perkins, R.D., Lukas, K.J., 1975. Boring microorganisms and microborings in carbonate substrates. In: Frey, R.W. (Ed.). The Study of Trace Fossils. Springer, New York, pp. 229–259.

Goldhammer, R.K., 1997. Compaction and decompaction algorithms for sedimentary carbonates. Journal of Sedimentary Research 67, 26-35.

Gordon, A.L., 2005. Oceanography of the Indonesian Seas and their Throughflow. Oceanography 18, 14-27.

Gradstein, F.M., Ogg, J.G., Smith, A.G., (Eds.), 2004. A Geologic Time Scale 2004, Cambridge University Press, UK. 589 pp.

Grainge, A.M., Davies, K.G. 1983. Reef exploration in the east Sengkang Basin, Sulawesi, Indonesia. 12th Annual Convention Indonesian Petroleum Association, Proceedings, 207-227.

Grötsch, J., Mercadier, C., 1999. Integrated 3-D Reservoir Modeling Based on 3-D Seismic: The Tertiary Malampaya and Camago Buildups, Offshore Palawan, Philippines. American Association of Petroleum Geologists, Bulletin 83, 1703-1728.

Guidry, S.A., Grasmueck, M., Carpenter, D.G., Gombos, A.M., Bachtel, S.L. and Viggiano, D.A. 2007. Karst and early fracture networks in carbonates, Turks and Caicos Islands, British West Indies. Journal of Sedimentary Research 77, 508-524.

Gunther, A., 1990. Distribution and bathymetric zonation of shell boring endoliths in recent reef and shelf environments: Cozumel, Yucatan (Mexico). Facies 22, 233–262.

Hall, R., 1996. Reconstructing Cenozoic SE Asia. In: Hall, R., Blundell, D.J. (Eds.), Tectonic Evolution of Southeast Asia. Geological Society of London Special Publication 106, pp. 153-184.

Hall, R., 2002a. Cenozoic geological and plate tectonic evolution of SE Asia and the SW Pacific: computer-based reconstructions, model and animations. Journal of Asian Earth Sciences 20(4), 353-431.

Hall, R., 2002b. SE Asian heat flow: Call for new data: Indonesian Petroleum Association Newsletter, 4, 20-21.

Hall, R., Wilson, M.E.J., 2000. Neogene sutures in eastern Indonesia. Journal of Asian Earth Sciences 18, 781–808.

Hall, R., Cottam, M.A. Wilson, M.E.J. (eds). 2011. The SE Asian gateway: history and tectonics of Australia-Asia collision. Geological Society of London, Special Publication 355, (381 pp).

Hamilton, W., 1979. Tectonics of the Indonesian region. United States Geological Survey Professional Paper 1078. (345 pp).

Halley, R.B., Scholle, P.A., 1985, Radiaxial fibrous calcite as early-burial, open-system cement: Isotopic evidence from Permian of China [abs.]. American Association of Petroleum Geologists Bulletin 69, 261.

Haq, B.U., Hardenbol, J., Vail, P.R. 1987. Chronology of fluctuating sea levels since the Triassic. Science 235, 1156-1165.

Hasan, K. 1991. The Upper Cretaceous flysch succession of the Balangbaru Formation, Southwest-Sulawesi. 20th Annual Convention Indonesian Petroleum Association Proceedings, 183-208.

Hendry, J.P., Taberner, C., Marshall, J.D., Pierre, C., Carey, P.F., 1999. Coral reef diagenesis records pore-fluid evolution and paleohydrology of a siliciclastic basin margin succession (Eocene South Pyrenean foreland basin, northeastern Spain): Geological Society of America, Bulletin, 111, 395-411.

Hudson, J.D., 1977. Stable isotopes and limestone lithification. Journal of the Geological Society of London 133, 637- 660.

Jones, B., Desrochers, A., 1992. Shallow Platform Carbonates. In: Walker, R.G., James, N.P. (eds.), Facies models, Response to sea level change. pp. 277-302.

Kuhnt, W., Holbourn, A., Hall, R., Zuvela, M., Käse, R., 2004. Neogene history of the Indonesian Throughflow. In: Clift, P., Wang, P., Kuhnt, W., Hayes, D.E. (Eds.).

Continent-Ocean Interactions within the East Asian marginal seas. AGU Geophysical Monograph 149, pp. 299-320.

Land, L. S., 1983, The application of stable isotopes to studies of the origin of dolomite and to problems of diagenesis of clastic sediments, *in* M. A. Arthur, T. F. Anderson, I. R. Kaplan, J. Veizer, and L. S. Land, (eds.) Stable Isotopes in Sedimentary Geology: SEPM Short course 10, p. 4-1 to 4-22.

Land, L.S., Moore, C.H., 1980. Lithification, micritization and syndepositional diagenesis of biolithites on the Jamaican Island slope. Journal of Sedimentary Petrology 50, 357-370.

Letouzey, J., Werner, P., Marty, A. 1990. Fault reactivation and structural inversion. Backarc and intraplate compressive deformations. Example of the eastern Sunda shelf (Indonesia). Tectonophysics 183, 341-362.

Lind, I.L. 1993. Stylolites in chalk from Leg 130, Ontong Java Plateau. In: Berger, W.H., Kroenke, L.W., Mayer, L.A. et al. (eds.). College Station (Ocean Drilling Program). Proceedings ODP Scientific Results, 130, 445-451,

Lunt, P., Allan, T., 2004. A history and application of larger foraminifera in Indonesian biostratigraphy, calibrated to isotopic dating. GRDC Workshop on Micropalaeontology, 109 pp.

Machel, H.G., 2004. Concepts and models of dolomitization: A critical reappraisal, in Braithwaite, Colin, J.R., Rizzi, G., Darke, G. (Eds.), The geometry and petrogenesis of dolomite hydrocarbon reservoirs. Geological Society of London Special Publication 235, pp.7–63.

Madden, R.H.C., Wilson, M.E.J., 2012. Diagenesis of delta-front patch reefs: a model for alteration of coastal siliciclastic-influenced carbonates from humid equatorial regions. Journal of Sedimentary Research 82, 871-888.

Madden, R.H.C., Wilson, M.E.J., 2013. Diagenesis of a SE Asian Cenozoic carbonate platform margin and its adjacent basinal deposits. Sedimentary Geology 286-287, 20-38.

Mayall, M.J., Cox, M., 1988. Deposition and diagenesis of Miocene limestones, Senkang Basin, Sulawesi, Indonesia. Sedimentary Geology 59, 77-92.

Mazzullo, J., Graham, A.J., (Eds.), 1988. Handbook for Shipboard Sedimentologists. ODP Technical Notes 8.

Moore, C.H., 1989. Carbonate diagenesis and porosity. Developments in Sedimentology 46. Elsevier. (338 pp).

Moore, C.H., 2001. Carbonate reservoirs, Porosity evolution and diagenesis in a sequence-stratigraphic framework. Developments in Sedimentology 55. Elsevier. (444 pp).

Moss, S.J and Chambers, J.L.C., 1999. Tertiary facies architecture in the Kutai Basin, Kalimantan, Indonesia. Journal of Asian Earth Science 17, 157-181.

Moss, S.J, Chambers, J., Cloke, I., Satria, D., Ali, J., Baker, S., Milsom, J. and Carter, A. 1997. New observations on the sedimentary and tectonic evolution of the Tertiary Kutai Basin, East Kalimantan. *In* Fraser, A.J., Matthews, S.J. and Murphy, R.W., (Eds.), Petroleum Geology of Southeast Asia. Special Publication of the Geological Society, London 126, 395-416.

Nicolaides, S., Wallace, M.W., 1997. Submarine cementation and subaerial exposure in Oligo-Miocene temperate carbonates, Torquay Basin, Australia. Journal of Sedimentary Research 67(3), 397-410.

Nelson, R. A. 1981. Significance of fracture sets associated with stylolite zones. American Association of Petroleum Geologists Bulletin 65 (11), 2417–2425.

Nelson, R. A. 2001. Geologic analysis of naturally fractured reservoirs. Gulf Professional Publishing, Butterworth–Heinemann, 2nd Edition, 163-222.

Peñaflor, E.L., Skirving, W.J., Strong, A.E., Heron, S.F., David, L.T., 2009. Sea-surface temperature and thermal stress in the Coral Triangle over the past two decades. Coral Reefs 28, 841-850.

Perry, C.T., 1998. Grain susceptibility to the effects of microboring: implications for the preservation of skeletal carbonates. Sedimentology 45, 39–51.

Perry, C.T., 1999. Biofilm-related calcification, sediment trapping and constructive micrite envelopes: a criterion for the recognition of ancient grass-bed environments? Sedimentology 46, 33–45.

Perry, C.T., Bertling, M., 2000. Spatial temporal patterns of macroboring within Mesozoic and Cenozoic coral reef systems. In: Skeleton, P.W., Insalaco, E., Palmer, T.J. (Eds.), Carbonate Platform Systems: Components and Interactions. Geological Society of London, Special Publication, 178, pp. 33–50.

Perry, C.T., Hepburn, L.J., 2008. Syn-depositional alteration of coral reef framework through bioerosion, encrustation and cementation: taphonomic signatures of reef accretion and reef depositional events. Earth-Science Reviews 86, 106–144.

Perry, C.T., Larcombe, P., 2003. Marginal and non-reef-building coral environments. Coral Reefs 22, 427–432.

Perry, C.T., Macdonald, I.A., 2002. Impacts of light penetration on the bathymetry of reef microboring communities: implications for the development of microendolithic trace assemblages. Palaeogeography Palaeoclimatology Palaeoecology 186, 101–113.

Pichler, T., Dix, G. R., 1996. Hydrothermal venting within a coral reef ecosystem, Ambitle Island, Papua New Guinea. Geology 5, 435–438.

Railsback, L. B., 1993. Lithologic controls on morphology of pressure-dissolution surfaces (stylolites and dissolution seams) in Paleozoic carbonate rocks from the mideastern United States. Journal of Sedimentary Research 63(3), 513-522.

Rosales, I., Fernandez-Mendiola, P.A., Garcia-Mondefar, J., 1994, Carbonate depositional sequence development on active fault blocks: the Albian in the Castro Urdiales area, northern Spain. Sedimentology 41, 861–882.

Saller, A., Armin, R., La Ode Ichram, C.G.S., 1992. Sequence stratigraphy of upper Eocene and Oligocene limestones, Teweh area, central Kalimantan. 21st Annual Convention Indonesian Petroleum Association Proceedings 1, 69-92.

Saller, A., Armin, R., Ichram, L.O., Glenn-Sullivan, C., 1993. Sequence stratigraphy of aggrading and back stepping carbonate shelves, Central Kalimantan, Indonesia. In: Loucks, R.G., Sarg, J.F. (Eds.), Carbonate sequence stratigraphy, recent developments and applications: American Association of Petroleum Geologists, Memoir, 57, pp. 267–290.

Saller, A.H., Vijaya, S. 2002. Depositional and diagenetic history of the Kerendan carbonate platform, Oligocene, central Kalimantan, Indonesia. Journal of Petroleum Geology 25, 123-150.

Sukamto, R., 1975. The structure of Sulawesi in the light of plate tectonics: Paper presented at Regional Conference on the Geology and Mineral Resources of SE Asia, Jakarta, pp. 1–25.

Sukamto, R., 1982. Geologi lembar Pangkajene dan Watampone bagian barat, Sulawesi: Geological Research and Development Centre, Bandung.

Sukamto, R., Supriatna, S., 1982, Geologi lembar Ujung Pandang, Benteng dan Sinjai quadrangles, Sulawesi: Geological Research and Development Centre, Bandung.

Swei, G.H., Tucker, M.E., 2012. Impact of diagenesis on reservoir quality in ramp carbonates: Gialo Formation (middle Eocene), Sirt Basin, Libya. Journal of Petroleum Geology 35, 25–48.

Swinchatt, J.P., 1965. Significance of constituent composition, texture, and skeletal breakdown in some recent carbonate sediments. Journal of Sedimentary Petrology 35, 71–90.

Taylor, J.M. 1950. Pore space reduction in sandstones. American Association of Petroleum Geologists Bulletin 34, 701-716.

Tomascik, T., Mah, A.J., Nontji, A., Moosa, M.K. 1997. The Ecology of the Indonesian Seas. Oxford University Press, Singapore, 1388 p.

Tucker, M.E., Wright, V.P., 1990. Carbonate Sedimentology. Blackwell Scientific Publications. (482 pp).

Vahrenkamp, V.C., David, F., Duijndam, P., Newall, M., Crevello, P. 2004. Growth architecture, faulting, and karstification of a Middle Miocene carbonate platform, Luconia province, offshore Sarawak, Malaysia. In: Eberli, G.P., Masafero, J.L., Sarg, J.F. (Eds.) Seismic imaging of carbonate reservoirs and systems. American Association of Petroleum Geologists Memoir 81, 329-350.

van de Vlerk, I.M., Umbgrove, J.H.F., 1927. Tertiaire gidsforaminifern van Nederlandsch Oost-Indiè. Wetensch. Meded. Dienst Mijnbouw Nederlandsch Oost-Indiè 6, 3-31.

van de Weerd, A.A., Armin, R.A., 1992. Origin and evolution of the Tertiary hydrocarbon bearing basins in Kalimantan (Borneo), Indonesia. American Association of Petroleum Geologists, Bulletin 76, 1778–1803.

van Geet, M., Swennen, R., Durmishi, C., Roure, F., Muchez, P.H. 2002. Paragenesis of Cretaceous to Eocene carbonate reservoirs in the Ionian fold and thrust belt (Albania): relation between tectonism and fluid flow. Sedimentology 49, 697–718.

van Leeuwen, T.M., 1981. The geology of southwest Sulawesi with special reference to the Biru area, in: Barber, A.J., Wiryosujono, S. (Eds.), The

Geology and Tectonics of Eastern Indonesia: Bandung, Geological Research and Development Centre, Special Publication, 2, pp. 277–304.

van Leeuwen, T.M., Susanto, E.S., Maryanto, S., Hadiwisastra, S., Sudijono, Muhardjo P., 2010. Tectonostratigraphic evolution of Cenozoic marginal basin and continental margin successions in the Bone Mountains, Southwest Sulawesi, Indonesia. Journal of Asian Earth Sciences 38, 233-254.

Wakita, K., Sopaheluwakan, J., Miyazaki, K., Zulkarnain, I., Munasri, 1996. Tectonic evolution of the Bantimala Complex, South Sulawesi, Indonesia. In Hall, R. Blundell, D.J. (eds.) Tectonic evolution of SE Asia. Geological Society, London, Special Publications 106, 353-364.

Wanless, H.R., Dravis, J.J., 1989. Carbonate environments and sequences of Caicos Platform. 28th International Geological Congress, Field Trip Guidebook, T374, (75 pp).

Warren, J., 2000. Dolomite: occurrence, evolution and economically important associations. Earth Science Reviews 52, 1-81.

Warrlich, G., Taberner, C., Asyee, W., Stephenson, B., Esteban, M., Boya-Ferrero, M., Dombrowski, A., Van Konijnenburg, J.-H. 2010. The impact of postdepositional processes on reservoir properties: two case studies of Tertiary carbonate buildup gas fields in Southeast Asia (Malampaya and E11). In: Morgan, W.A., George, A.D, Harris, P.M., Kupecz, J.A., Sarg, J.F. (Eds.). Cenozoic Carbonate Systems of Australasia. SEPM (Society for Sedimentary Geology), Special Publication 95, 99-127.

Wilson, M.E.J. 1995. The Tonasa Limestone Formation, Sulawesi, Indonesia: Development of a Tertiary Carbonate Platform. Unpublished Ph.D. Thesis, University of London, 520 p.

Wilson, M.E.J., 1996. Evolution and hydrocarbon potential of the Tertiary Tonasa Limestone Formation, Sulawesi, Indonesia. Proceedings of the Indonesian Petroleum Association 25th Annual Convention, 227-240.

Wilson, M.E.J., 1999. Prerift and synrift sedimentation during early fault segmentation of a Tertiary carbonate platform, Indonesia. Marine and Petroleum Geology 16(8), 825-848.

Wilson, M.E.J., 2000. Tectonic and volcanic influences on the development and diachronous termination of a Tertiary tropical carbonate platform. Journal of Sedimentary Research 70(2), 310-324.

Wilson, M.E.J. 2002. Cenozoic carbonates in SE Asia: Implications for equatorial carbonate development. Sedimentary Geology 147, (3-4), 295-428.

Wilson, M.E.J., 2008. Global and regional influences on equatorial shallow marine carbonates during the Cenozoic. Palaeogeography, Palaeoclimatology, Palaeoecology 265, 262–274.

Wilson, M.E.J., 2012. Equatorial carbonates: an earth systems approach. Sedimentology 59, 1–31.

Wilson, M.E.J., Bosence, D.W.J., 1996. The Tertiary evolution of South Sulawesi: a record in redeposited carbonates of the Tonasa Limestone Formation. In Hall, R. Blundell, D.J. (eds.) Tectonic evolution of SE Asia. Geological Society, London, Special Publications 106, 365-389.

Wilson, M.E.J., Bosence, D.W.J., 1997. Platform top and ramp deposits of the Tonasa Carbonate Platform, Sulawesi, Indonesia. In: Fraser, A., Matthews, S.J., Murphy, R.W. (Eds.), Petroleum Geology of SE Asia, Geological Society of London, Special Publication 126, pp. 247–279.

Wilson, M.E.J., Evans, M. J., 2002. Sedimentology and diagenesis of Tertiary carbonates on the Mangkalihat Peninsula, Borneo: Implications for subsurface reservoir quality. Marine and Petroleum Geology 19, 873 – 900.

Wilson, M.E.J., Hall, R., 2010. Tectonic influence on SE Asian carbonate systems and their reservoir quality. In: Morgan, W.A., George, A.D., Harris, P.M., Kupecz, J.A. Sarg, J.F. (Eds.), Cenozoic Carbonate Systems of Australasia. SEPM, Special Publication 95, pp. 13–40.

Wilson M.E.J., Rosen, B. R., 1998. Implications of the paucity of corals in the Paleogene of SE Asia: plate tectonics or centre of origin? In: Hall, R.H. (Eds.), Biogeography and geological evolution of SE Asia. Backhuys Publishers, Leiden, pp. 165–195

Wilson, M.E.J. Vecsei, A., 2005. The apparent paradox of abundant foramol facies in low latitudes: their environmental significance and effect on platform development. Earth Science Reviews 69, 133–168.

Wilson, M.E.J., Bosence, D.W.J., Limbong, A., 2000. Tertiary syntectonic carbonate platform development in Indonesia. Sedimentology 47(2), 395-419.

Wilson, M.E.J., Chambers, J.L.C, Evans, M.J., Moss, S.J., Satria Nas, D., 1999. Cenozoic carbonates in Borneo: Case studies from Northeast Kalimantan. Journal of Asian Earth Science 17, 183-201.

Wilson, M.E.J., Chambers, J.L.C., Manning, C., Nas, D.S. 2012. Spatio-temporal evolution of a Tertiary carbonate platform margin and adjacent basinal deposits. Sedimentary Geology 271-272, 1-27.

Wilson, M.E.J., Chang, E.E.W., Dorobek, S., Lunt, P. 2013. Onshore to offshore trends in carbonate sequence development, diagenesis and reservoir quality across a land-attached shelf in SE Asia. Marine and Petroleum Geology 45, 349-376.

Witkowski, F.W., Blundell, D.J., Gutteridge, P., Horbury, A.D., Oxtoby, N.H., Qing, H., 2000. Video cathodoluminescence microscopy of diagenetic cements and its applications. Marine and Petroleum Geology 17, 1085-1093.

Yuwono, Y.S., Maury, R.C., Soeria-Atmadja, P., Bellon, H., 1987. Tertiary and Quaternary geodynamic evolution of South Sulawesi: Constraints from the study of volcanic units. Geologi Indonesia 13, 32–48.

Zampetti, V., Schlager, W., Van Konijenburg, J.H., and Everts, A.J., 2003. Depositional history and origin of porosity in a Miocene carbonate platform of central Luconia, offshore Sarawak: Bulletin of the Geological Society of Malaysia, 47, 139-152.

Figures and Tables

Figure 1. Regional tectonic setting of Sulawesi and the location of the Tertiary basinal area in Sulawesi/Borneo (from Wilson et al., 2000, modified after Daly et al., 1991; Hall, 1996; van de Weerd and Armin, 1992; Wilson, 1999). Inset shows the position of the research area within Sulawesi.

Figure 2. Geological map of South Sulawesi (from Wilson et al., 2000; after van Leeuwen, 1981; Sukamto, 1982; Sukamto and Supriatna, 1982; Wilson, 2000), showing the locations of the five main outcrop areas of the Tonasa Formation and the location of mentioned measured sections.

Figure 3. Selected summary measured sections from north to south across the main Tonasa tilt-block platform with diagenetic summaries from petrography of individual samples plotted against logged sections from Wilson et al. (2000) and Wilson (1995).

Figure 4. Selected summary measured sections from west to east across areas of complex block faulting in the Tonasa carbonate platform with diagenetic summaries from petrography of individual samples plotted against logged sections from Wilson et al. (2000) and Wilson (1995).

Figure 5. Thin-section plane polarised light photomicrographs showing (a) Micrite envelope (arrowed) encircling gastropod, the latter replaced by ferroan calcite (CG10, Eastern Area). (b and c) Micritic envelopes (arrowed), 20-30 μm thick, in coral floatstone from the Central Area (GC10). Coral skeleton is replaced by granular mosaic cement, whereas micritised cavity in coral arrowed in 'b' contains a partial micritic geopetal infill followed by bladed then blocky cement infill. (d) Imperforate foraminifera-rich

grainstone from the central area (GC9) showing grain distortion of micritic-walled miliolids. Syntaxial overgrowth on echinoderm has a concavo-convex contact with adjacent distorted miliolid. Cement between grains is predominantly granular mosaic calcite, some including 'dusty' micritic areas. (e) Tangential to sutured grain contacts in shallow water larger benthic foraminifera bioclastic packstone from the Western Area (P18e). Mechanical breakage of the thin discocyclinids is common, whereas the robust *Pellatispira/?Biplanispira* (centre left) and *Nummulites* (centre right) act more like indentor grains having slightly sutured contacts with surrounding allochems. (f) Concavo-convex to sutured grain contacts in shallow water bioclastic packstone from the Eastern Area (SRa52), with swarm-like bed-parallel stylolites to dissolution seams.

Figure 6: Thin-section photomicrographs of pore-lining cements from the Tonasa Platform. (a) Possible bladed to isopachous grain fringing cement with slightly micritised crystal terminations (black arrows), now replaced by granular mosaic cement (Eastern Area, CG9). (b and c) 'Turbid' radiaxial fringing cement lining cavities between bioclasts and post-dating minor clear isopachous fringing cement. Radiaxial cements are up to 2 mm long and show sweeping extinction patterns within crystals, when viewed from perpendicular to the long axis of the crystal under cross-polarised light. Radiaxial cements are post-dated by partial micritic infill in cavities then clear equant to blocky calcite cement. post-dating cavities between bioclasts (Western area, SMa26c). (d) Bladed dark-pink stained, non-ferroan calcite lining irregular dissolutional cavities (arrowed). Silt-sized rhombs of dolomite (colourless) partially infill remaining pore space, with a later phase of pale-pink stained equant calcite cement infilling the remainder of the pore space (Northern area, SM^9). (e) Bladed

non-ferroan cement lining intergranular pore space (arrowed). Bladed cement is pre-dated by a 'turbid' isopachous cement fringing grains (now replaced by granular mosaic cement), giving the pore-lining cements a banded appearance. Later blocky cement partially infills pore space (Western area, SMa11). (f) 'Turbid' bladed to banded cement partially infilling irregular fracture to dissolutional cavity. Bladed cement is preceded by an earlier dogtooth to blocky cement (arrowed) and micritic sediment infill. Equant to blocky cement infills later cross-cutting fractures and remaining cavity pore space (Eastern area, CG9). (g) Scalenohedral to dogtooth calcite (arrowed) lining irregular cavity. Cavity is infilled by micrite of varying darkness, with minor later blocky cement (Northern area, SP32). (h) Cathodoluminescene image with majority of image showing very dull luminescent micritic-rich sample. Curved mold after fragmented shell in right of image has blocky cement with non-luminescent character and a bright luminescent fringe. This is followed by dull luminescent pore filling cement in both the centre of the shell biomold and also the fracture, the latter in the left of the image. Non-luminescent areas within the pore filling cement areas are minor porosity, some possibly due to cement plucking during thin sectioning (Eastern area, CG7).

Figure 7. (a) Probable Tertiary karstic dissolution cavity infilled in fine sediment "s" and banded calcite cement "c". (b) Photomicrograph of Miocene karstic fissure-fill sediment (including cave pearls) from the uppermost part of the Tonasa Formation in the Camba section from the eastern area. Scale bar: 0.5 mm. Laminae of micrite and cave pearls constitute most of the cavity fill. A fracture infilled with fine volcaniclastic sediment post-dates the carbonate fill of the cavity (right side of image).

Figure 8. Thin-section photomicrographs show syntaxial overgrowth cements from the Tonasa Platform. (a) Clear to slightly turbid syntaxial overgrowth cement under plane polarised light in quartzose bioclastic grainstone (SMa11). Syntaxial overgrowths post-date some mechanical compaction. (b and c) Syntaxial overgrowth cements up to 1 mm thick on echinoderm material. Overgrowth cements post-date some compaction (black arrows show cement growth after grain fracturing; GC3). (d) Cathodoluminescent image (S13a) and (e and f) plane polarised light and cathodoluminescent image pair (S10a) showing CL cement zonation not visible under plane light. Sequence of CL luminescence: (1) dull-, (2) non-, (3) bright-, to (4) bright to dull-luminescent.

Figure 9. Thin-section photomicrographs show varied cement phases and fracturing from the Tonasa Platform. (a) Granular mosaic to blocky cement with clear irregular/subhedral crystal (SC6b). (b) Ferroan granular mosaic calcite replacing bioclast (1), cut by fracture, with bladed to blocky cement infilling fracture (2; MC2). (c) Pale blue stained (ferroan) granular mosaic to equant calcite replacing bioclast and micritic infill (top right), and infilling intragranular and early fracture porosity. Later fracture cross cutting all earlier features is filled by a granular mosaic to equant cement stained a darker blue than the earlier ferroan calcite (SMa47). (d) Clear, ferroan (blue-stained) granular mosaic calcite 'in place' of non-calcitic bioclasts. (e) Ferroan granular mosaic to blocky calcite replacing bioclasts (ghost texture of original wall structure preserved) and infilling adjacent porosity (BM36). Most visible in upper part of image infilled by ferroan granular mosaic cement. (f) Sub-millimetre and millimetre-scale fractures infilled by equant to blocky cements (CG9).

Figure 10. Thin-section photomicrographs showing fracturing and pore-filling cements from the Tonasa Platform. (a and b) Plane polarised light and cathodoluminescent image pair showing fracture filled by granular mosaic to equant cement (yellow arrow) and cut by other fracture with another equant cement associated with stylolites (white arrow; Sample SMa47). CL image highlights different relative timing of fracturing and their cementation. (c) Displacement along irregular fracture (SMa24). (d and e) Predominantly euhedral crystals of equant to blocky cement (up to 800 µm; LB2 and UL3, respectively). (f) Drusy to blocky cements in intragranular and biomoldic porosity after coral (CG10). Thin section photomicrograph cuts across the half stained part of the thin section (stained area to right). Micrite envelope to original coral is seen top right and part of the micritic, slightly peloidal chamber infill of the coral is seen bottom left.

Figure 11. Map of South Sulawesi showing structural trends (after Sukamto, 1982; Sukamto and Supriatna, 1982; Wilson, 1995). The orientations of near vertical large-scale faults, resolvable on geological maps, from the different areas of South Sulawesi have been plotted as rose diagrams. Dip directions of faults were commonly not given on the geological maps (cf. Sukamto, 1982; Sukamto and Supriatna, 1982), consequently the strike direction of faults has been plotted as bi-directional data. The dominant fault trends in South Sulawesi are NW-SE and NNW-SSE. The numbers of small-scale fractures and/or calcite filled veins, resolvable at the outcrop scale with apertures on a centimetre to millimetre scale, for the different areas of the Tonasa Limestone Formation are plotted as radial scatter plots. Dip information for near-vertical small-scale structures was recorded in the field, consequently the strike direction of the feature is recorded uni-directionally with planar feature dipping at

ninety degrees clockwise to the recorded strike direction (i.e. the 'right-hand rule'). The dominant small-scale fracture and vein trends in the Tonasa Limestone Formation are NW(-SE) and NNW(-SSE), with subsidiary trends to the NE(-SW) and NNE-SSW.

Figure 12. Fracture distribution and evidence for their relative timing from a study of 164 thin sections across all areas of the Tonasa Formation. (a) Ratios of numbers of highly irregular and straight fractures to the numbers of samples studied from in place, mostly shallow-water, deposits. (b) Ratios of numbers of fractures within clasts to the numbers of samples studied from sediment gravity flow deposits, with clast sizes greater than 5 mm, from the northern, eastern and western areas. Abbreviations are after the section names in the main different areas of the Tonasa Formation.

Figure 13. Thin-section photomicrographs showing pore infilling cements, stylolites/dissolution seams and dolomite from the Tonasa Platform. (a) CL image of predominantly non-luminescent blocky pore-infilling cement with some bright zones (SMa26c). (b) Irregular stylolites to dissolution seam with concentration of insolubles along sutured interface (CG7). (c) Anastomosing dissolution seams (concentrating insolubles) and grain-scale compaction (MC1). (d) 'Dusty' to clear, intergranular rhombic dolomite crystals (GC25). (e and f) Plane polarised light and CL image pair of fully dolomitised sample for the central area (GC58). Dusty interior to dolomite rhombs is non-luminescent with brighter 'flecks'. Clear dolomite cements forming the edges of the rhombs shows faint bright, dull, bright luminescence.

Figure 14. Stable isotope plot ($\delta^{18}O$ versus $\delta^{13}C$ ‰ V-PDB) of carbonate allochems, cements and matrix from the Tonasa Limestone Formation.

Figure 15. Generalised paragenetic sequence inferred for the Tonasa Limestone Formation. Relative timing of diagenetic features is inferred from petrography, but may vary slightly between samples. See text for further details on the interpreted diagenetic environment.

Figure 16. Schematic palaeoreconstruction of the main north-south trending Tonasa tilt-block platform for the Oligocene or Early Miocene (after Wilson et al., 2000). Cartoons summarise main diagenetic features affecting different parts of the platform. In general, cartoons above the reconstruction show diagenesis in shallow burial depths, whereas the overprint of deeper burial diagenesis is added on those below the main figure.

Table 1. Stable isotope results ($\delta^{18}O$ and $\delta^{13}C$ ‰ V-PDB) of analysis of carbonate allochems, cements and matrix from the Tonasa Limestone Formation.

Table

Sample	Area/Fm.	Delta 13C	Delta 18O	18OSMOW	New names
P18e	Western Area	1.96	-3.59	27.21	Larger benthic foraminifera - Nummulites
WM9	Eastern Area	1.79	-13.86	16.62	Larger benthic foraminifera - Nummulites
SP43	Northern Area	-9.11	-14.20	16.27	Larger benthic foraminifera - Nummulites
DD1	Northern Area	-10.90	-16.05	14.36	Larger benthic foraminifera - Nummulites
DD46b	Northern Area	1.81	-4.57	26.20	Larger benthic foraminifera - Nummulites
TII-1	Central Area	-2.04	-6.28	24.44	Larger benthic foraminifera - Nummulites & ?minor micrite
LB6	Eastern Area	0.28	-6.40	24.32	Larger benthic foraminifera - Nummulites & ?minor micrite
TII-68	Central Area	0.88	-5.45	25.29	Larger benthic foraminifera - Lepidocyclina
TII-47	Central Area	-2.23	-7.60	23.08	Larger benthic foraminifera - Lepidocyclina
DD111	Northern Area	1.20	-1.71	29.15	Larger benthic foraminifera - Lepidocyclina
BBu25	Northern Area	0.65	-2.51	28.32	Larger benthic foraminifera - Lepidocyclina
TII-49a	Central Area	-2.67	-7.35	23.34	Algal laminite - algal 'sparry' layer
TII-49b	Central Area	-3.40	-6.82	23.88	Algal laminite - micritic layer
SMa26ca	Western Area	2.09	-3.64	27.15	Pore-lining radiaxial fringing cement
CG6a	Eastern Area	1.98	-6.54	24.17	Scalenohedral to dogtooth cement lining dissolution cavity
SMa26cb	Western Area	-0.21	-6.45	24.26	Micritic cavity infill (after radiaxial fringing cement)
CG6b	Eastern Area	-13.46	-18.85	11.46	Micritic infill within dissolution cavity
CG7	Eastern Area	1.18	-5.68	25.06	Micritic sediment interbedded with cave pearls
P7a	Western Area	1.69	-5.46	25.28	Granular mosaic to equant calcite between grains
P7b	Western Area	2.38	-9.47	21.14	Granular mosaic to equant calcite between grains
BM7a	Eastern Area	2.37	-8.32	22.33	Blocky to equant calcite cement replacing coral
BM7b	Eastern Area	-0.14	-4.01	26.78	Blocky to equant calcite cement between grains
DD45	Northern Area	-14.23	-19.68	10.62	Blocky calcite cement between grains
DD46a	Northern Area	1.22	-5.65	25.09	Blocky calcite cement between grains
R2	Northern Area	-9.45	-17.43	12.94	Equant cement replacing bioclasts
DD29	Northern Area	0.35	-7.12	23.57	Blocky calcite cement filling fracture
R7	Northern Area	1.97	-4.50	26.27	Blocky calcite cement filling fracture
WP1	Eastern Area	1.22	-7.72	22.95	Blocky calcite cement filling fracture
UL3	Eastern Area	1.18	-6.28	24.43	Blocky calcite cement filling fracture
CG9	Eastern Area	0.16	-5.00	25.76	Non Ferroan blocky calcite fracture fill
ST16	Northern Area	-0.30	-4.05	26.73	Ferroan equant to blocky calcite fracture fill
GC58	Central Area	1.90	-3.70		Replacive cloudy dolomite
GC52a	Central Area	2.00	-5.30		Replacive cloudy dolomite
GC52b	Central Area	2.10	-4.60		Replacive cloudy dolomite
GC30	Central Area	-0.40	-2.70		Replacive cloudy dolomite
GC25	Central Area	-0.60	-3.30		Replacive cloudy dolomite

Figure 1

Figure 1

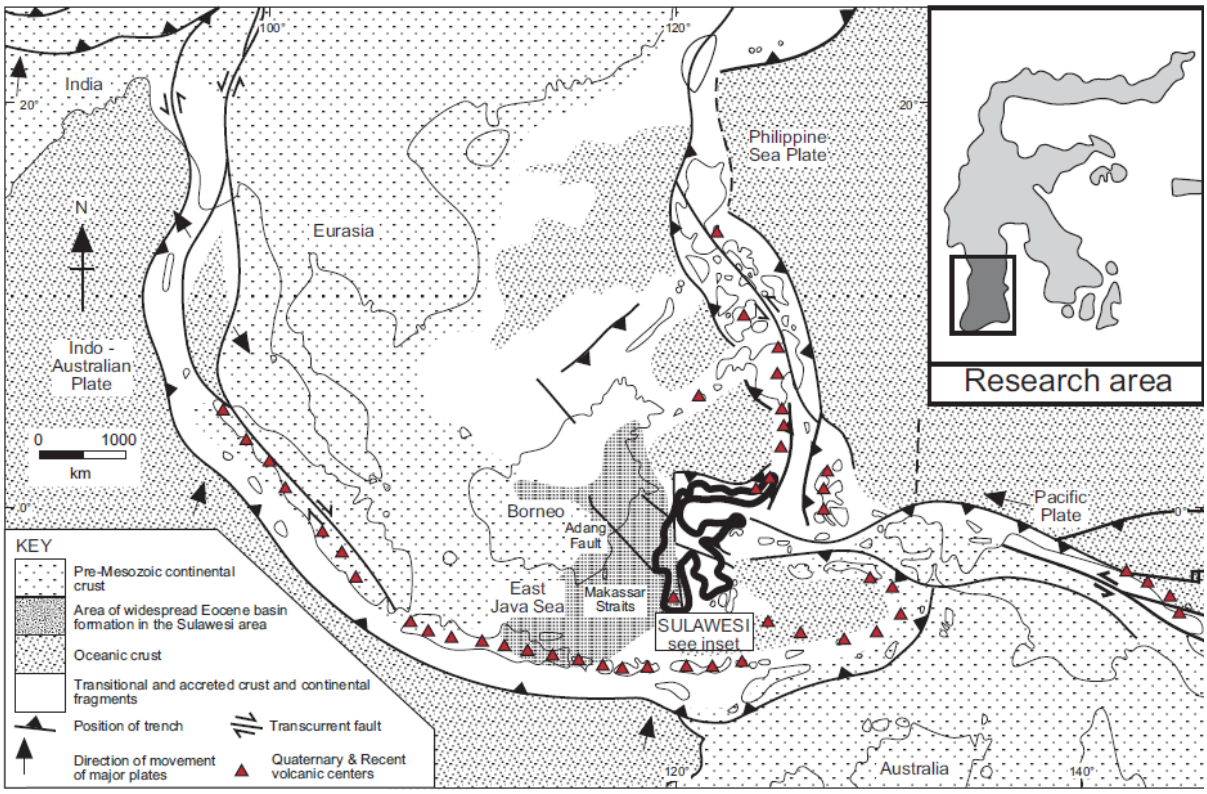

Figure 2

Figure 2

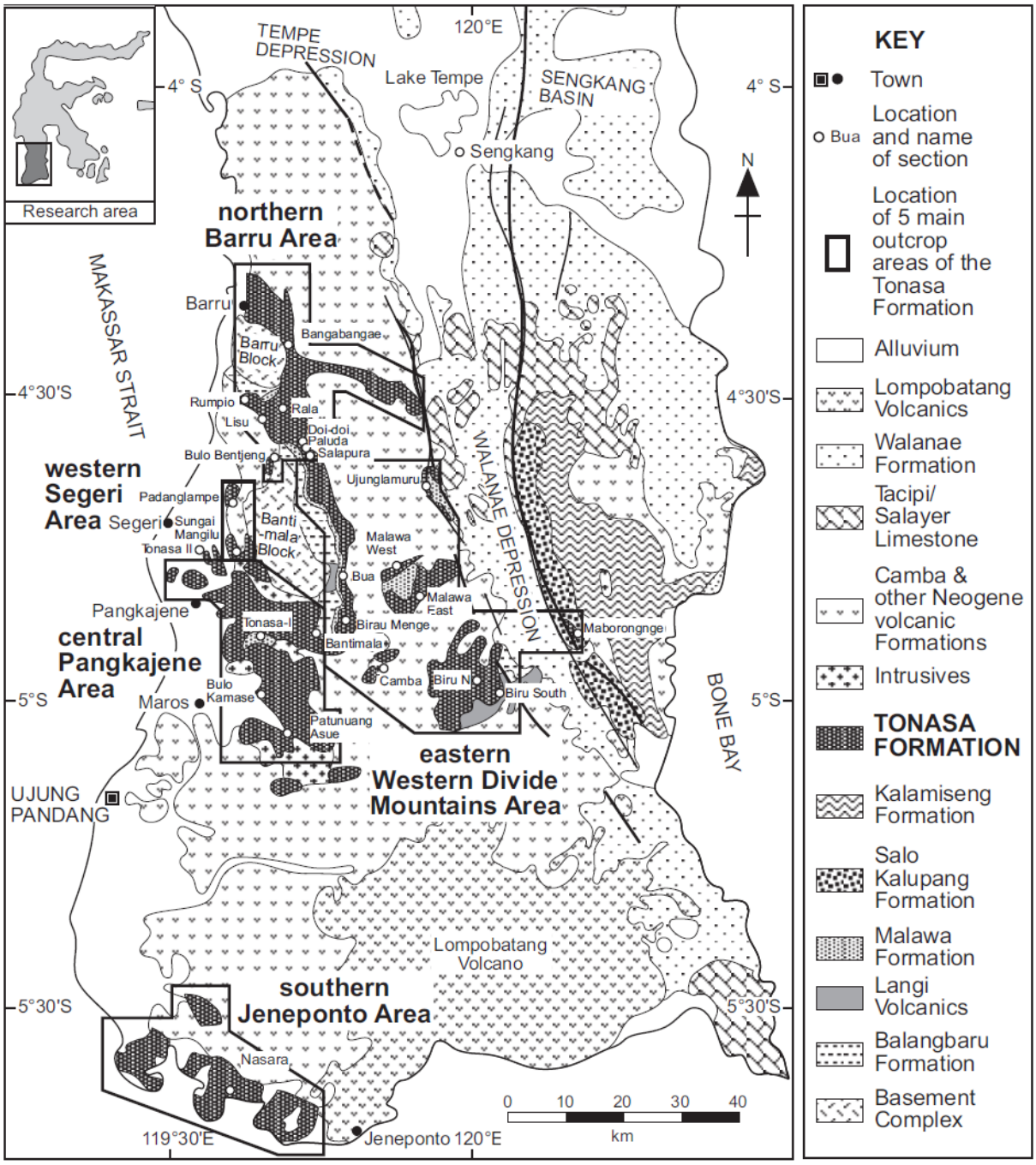

Figure 3

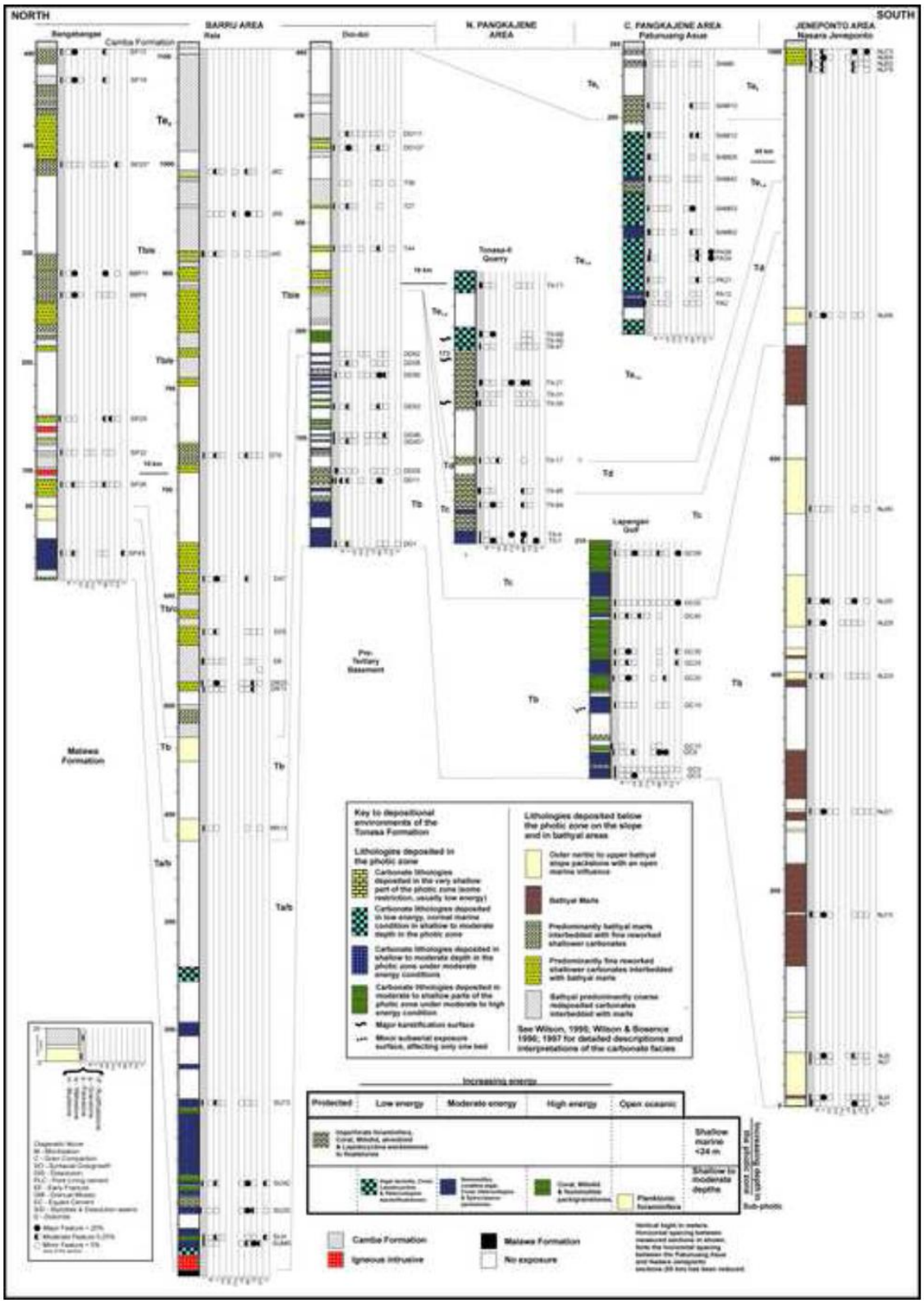

Figure 4

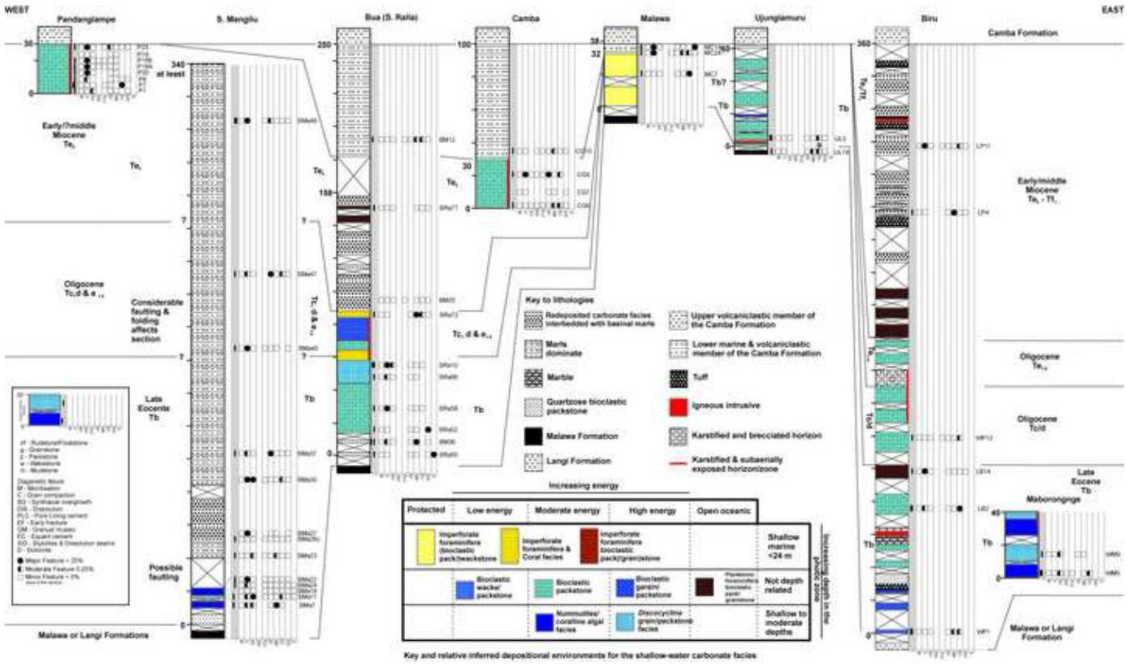

Key and relative inferred depositional environments for the shallow-water carbonate facies

Figure 5

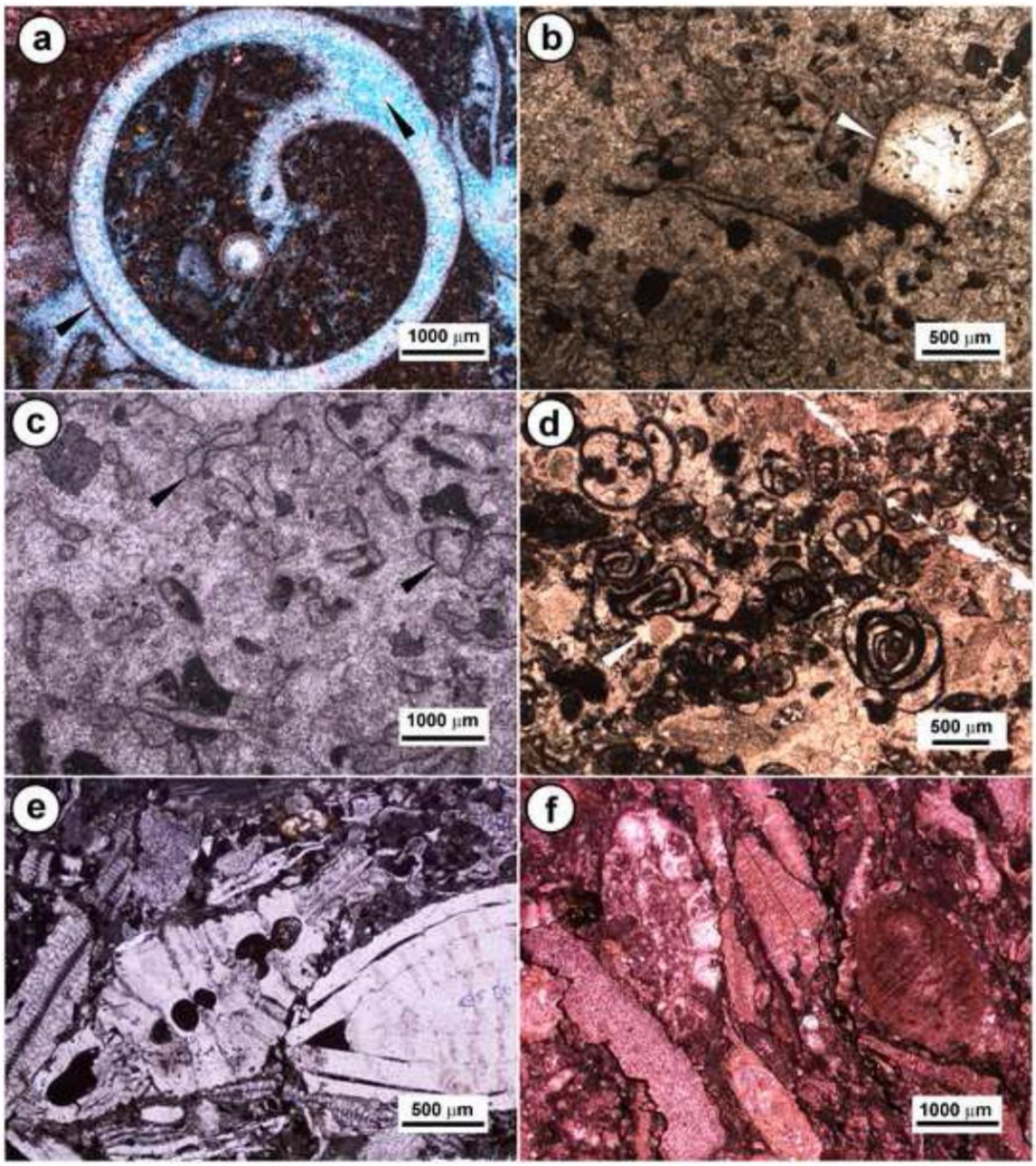

Figure 6

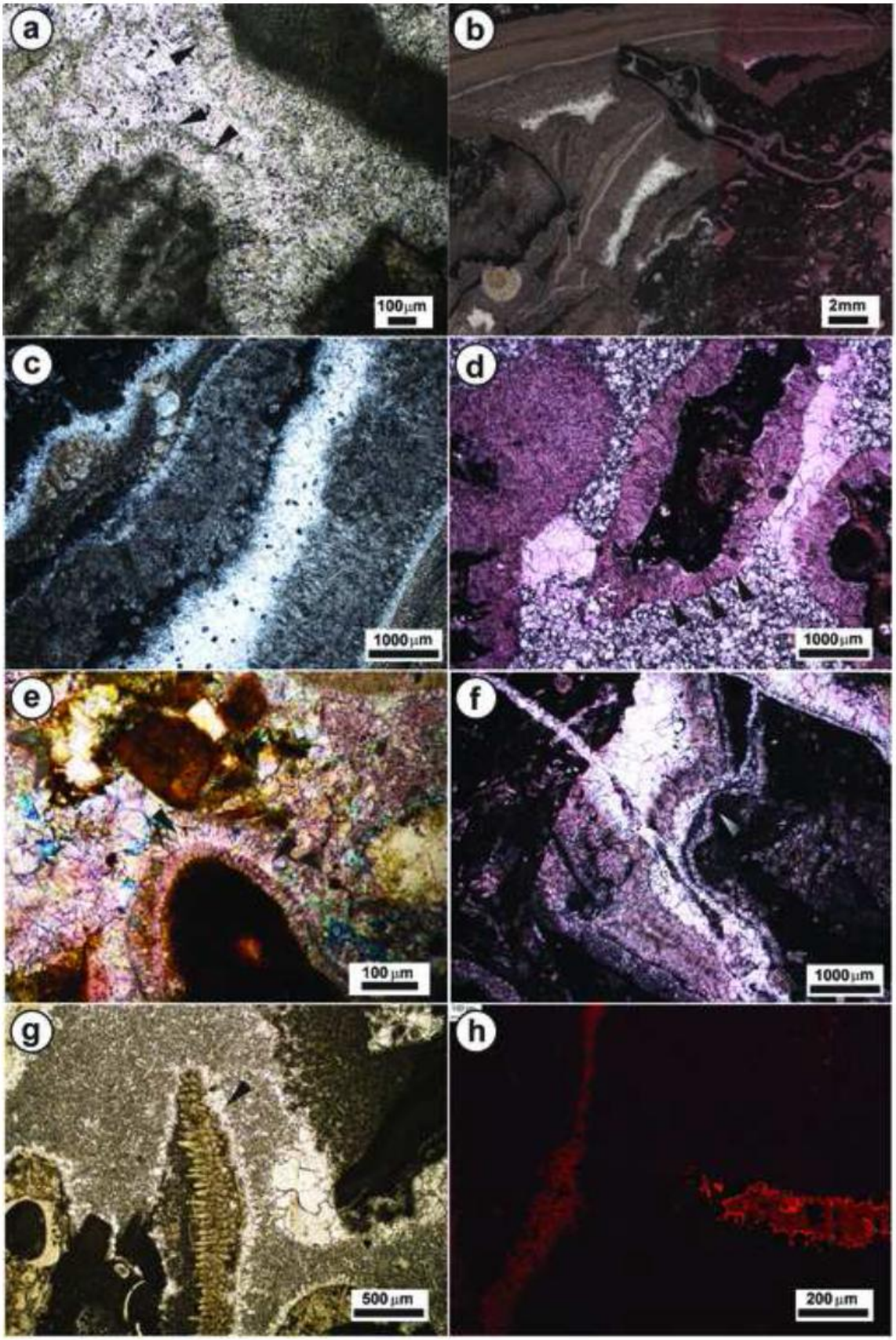

Figure 7

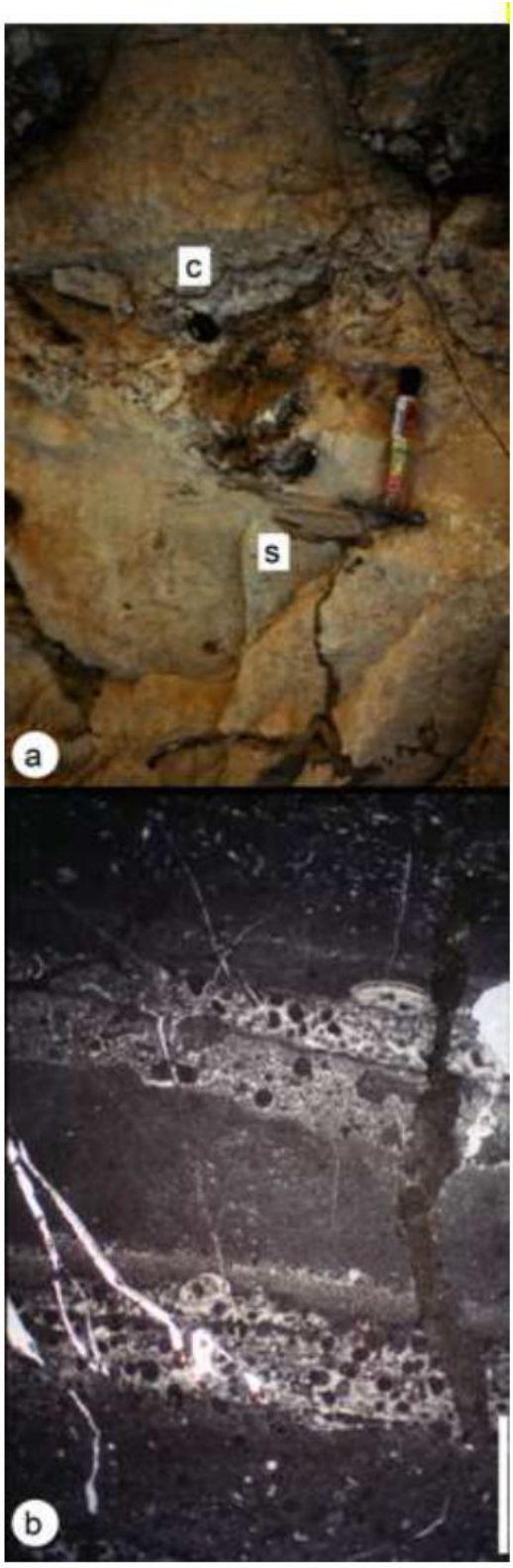

Figure 8

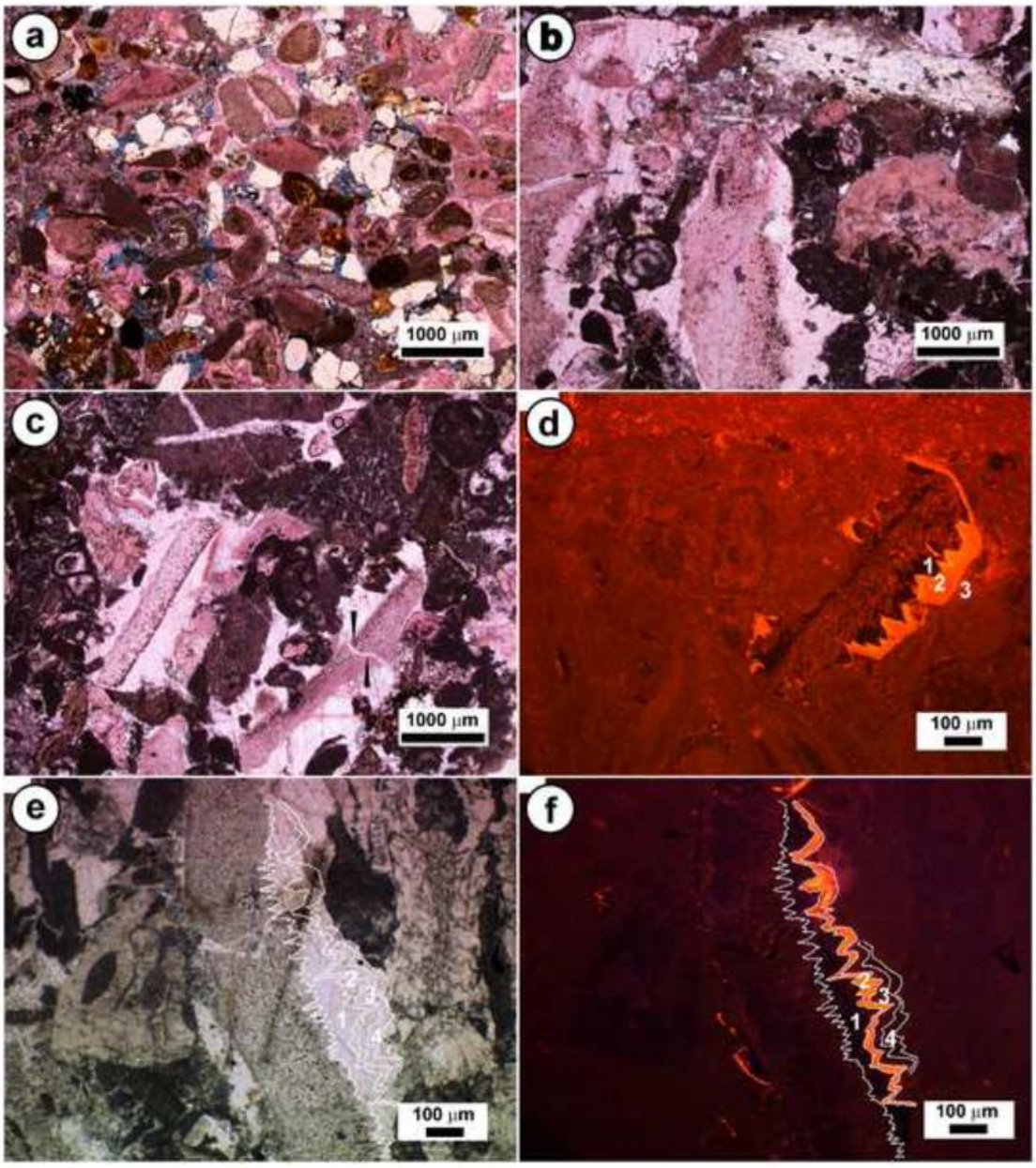

Figure 9

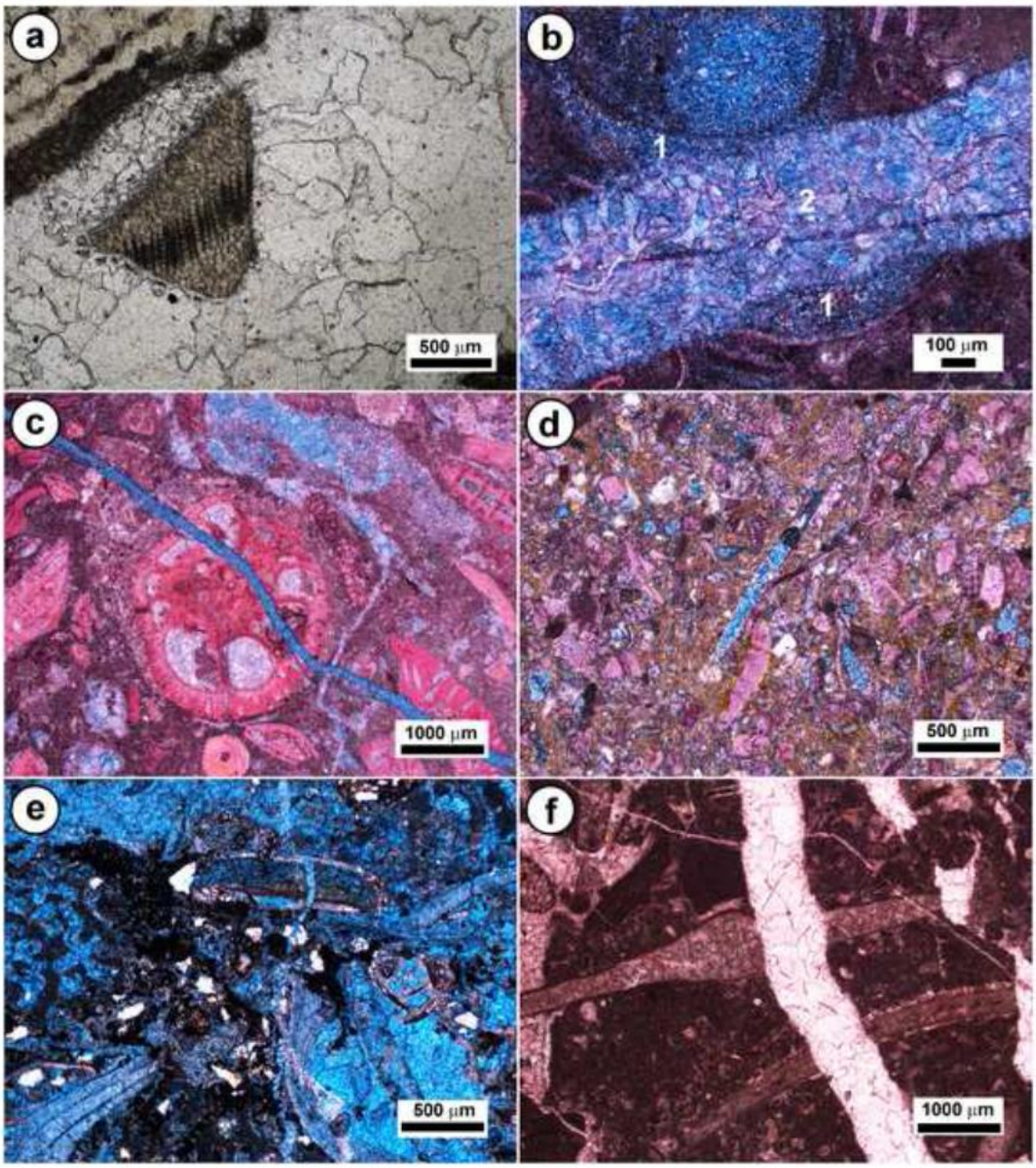

Figure 10

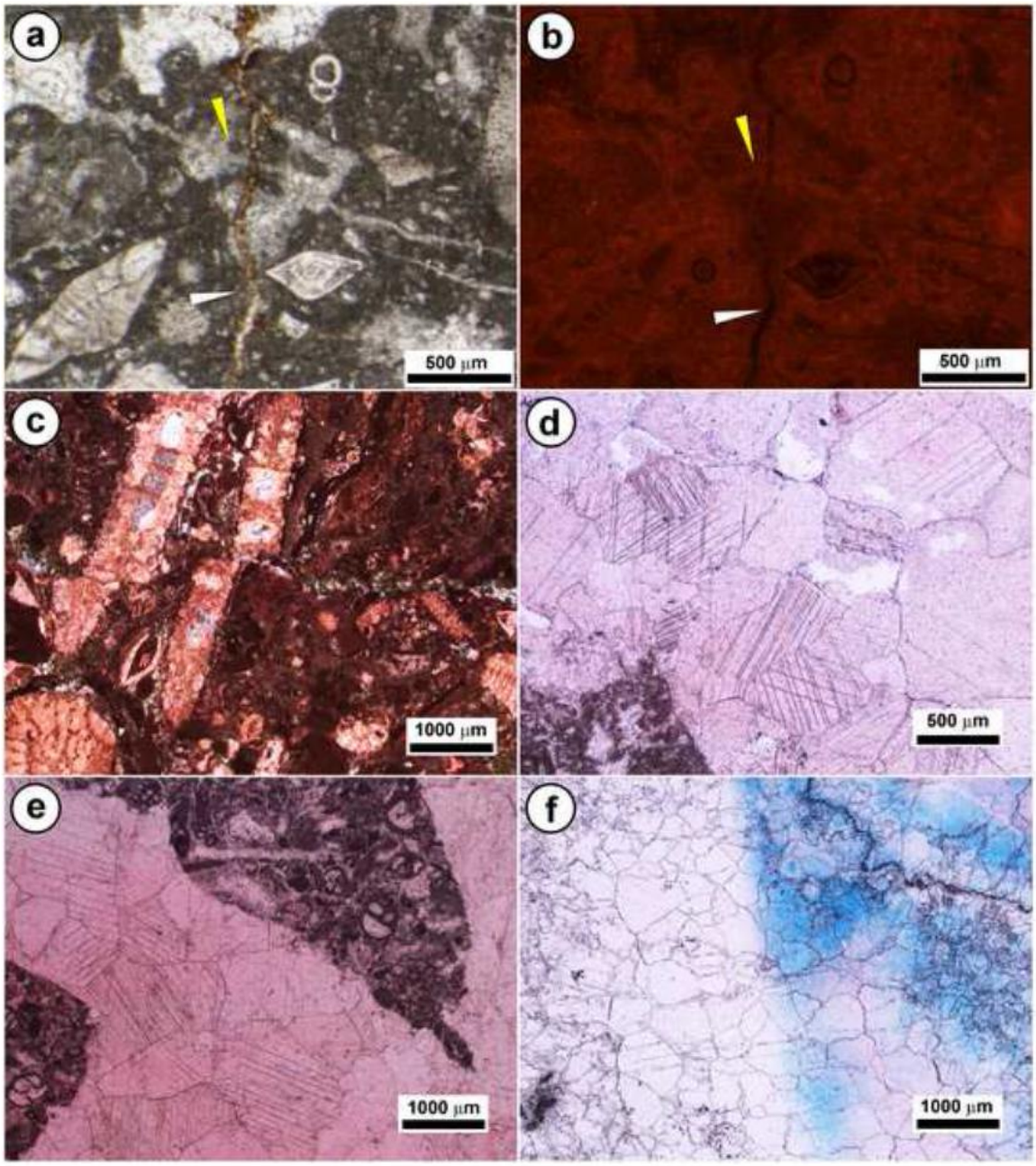

Figure 11

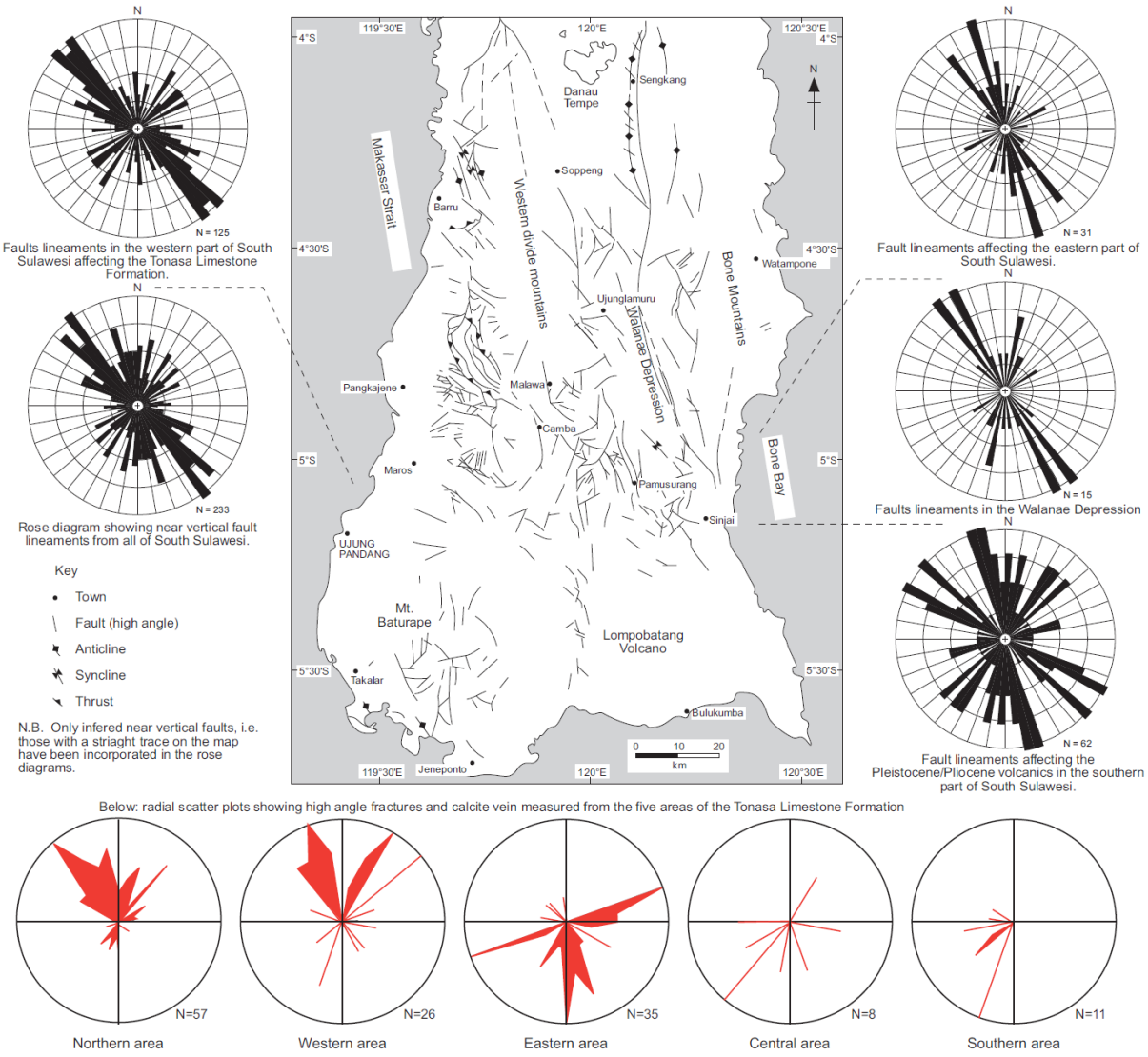

Figure 12

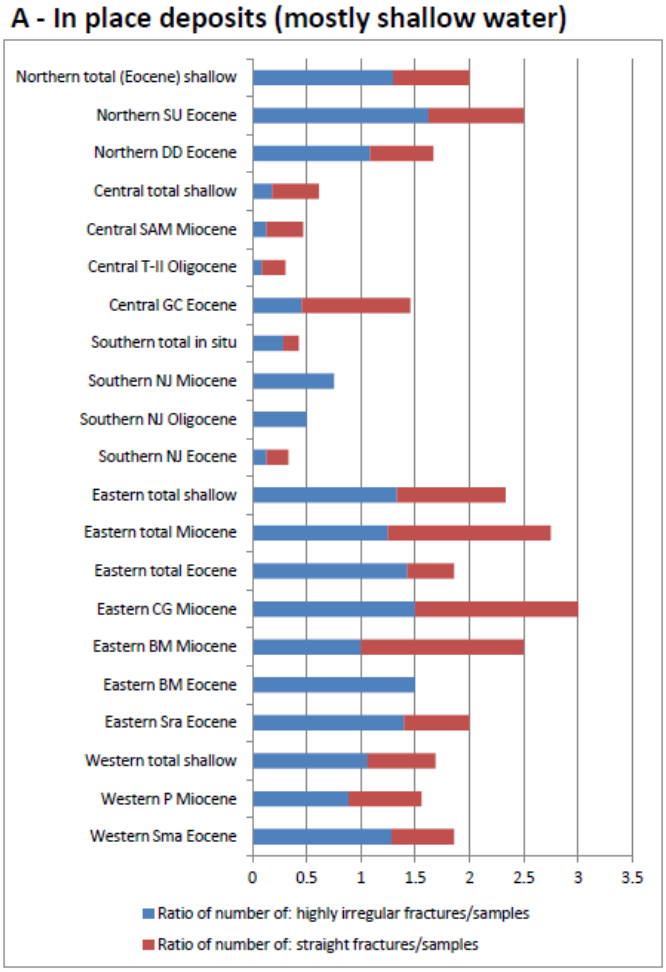

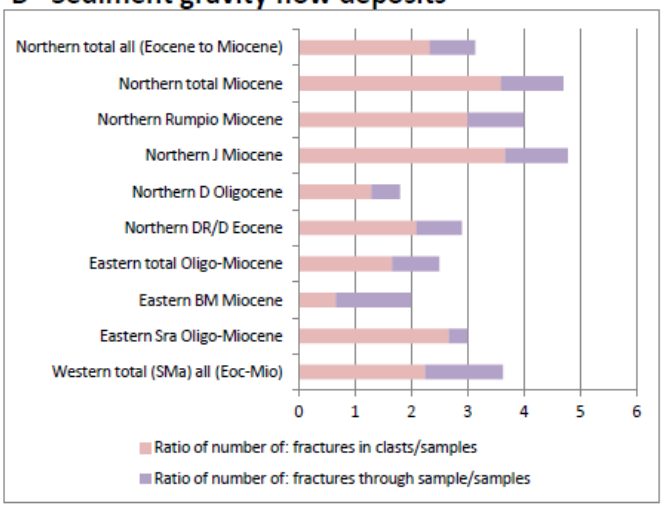

Figure 13

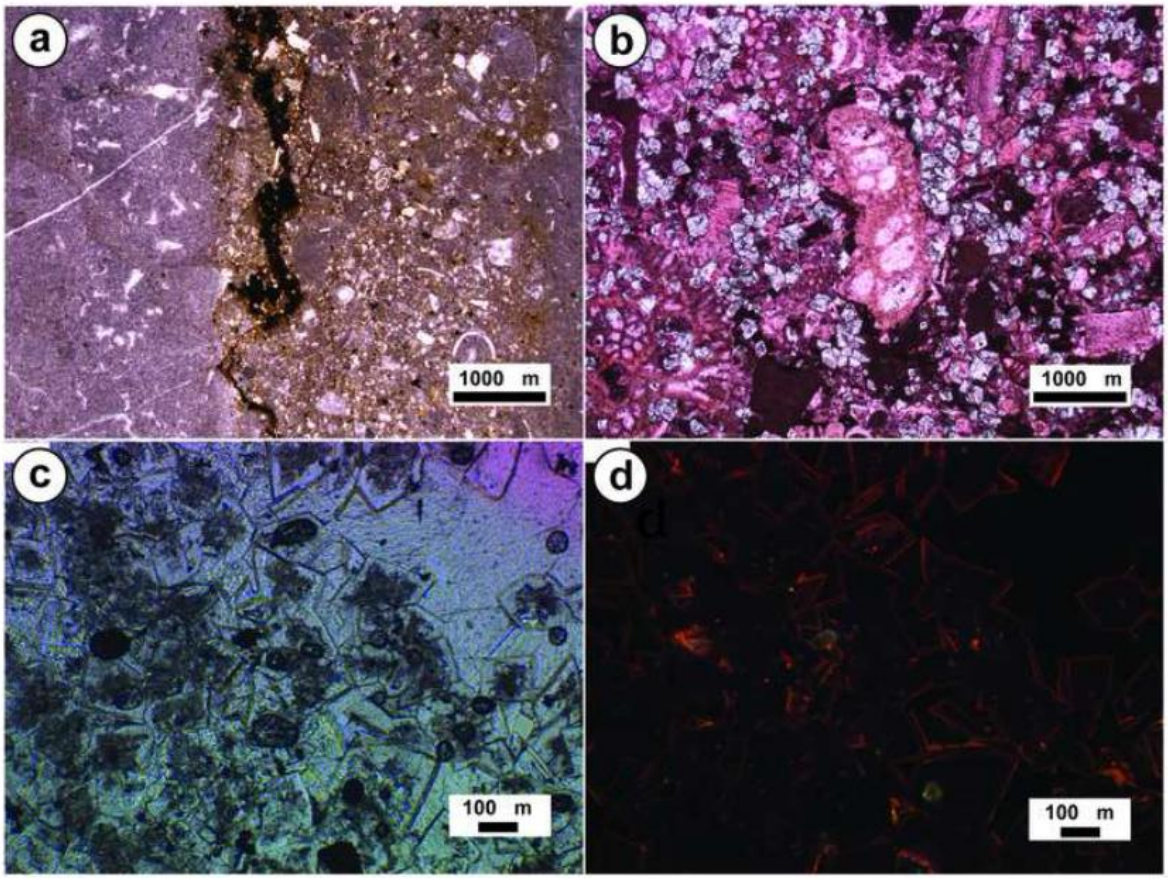

Figure 14

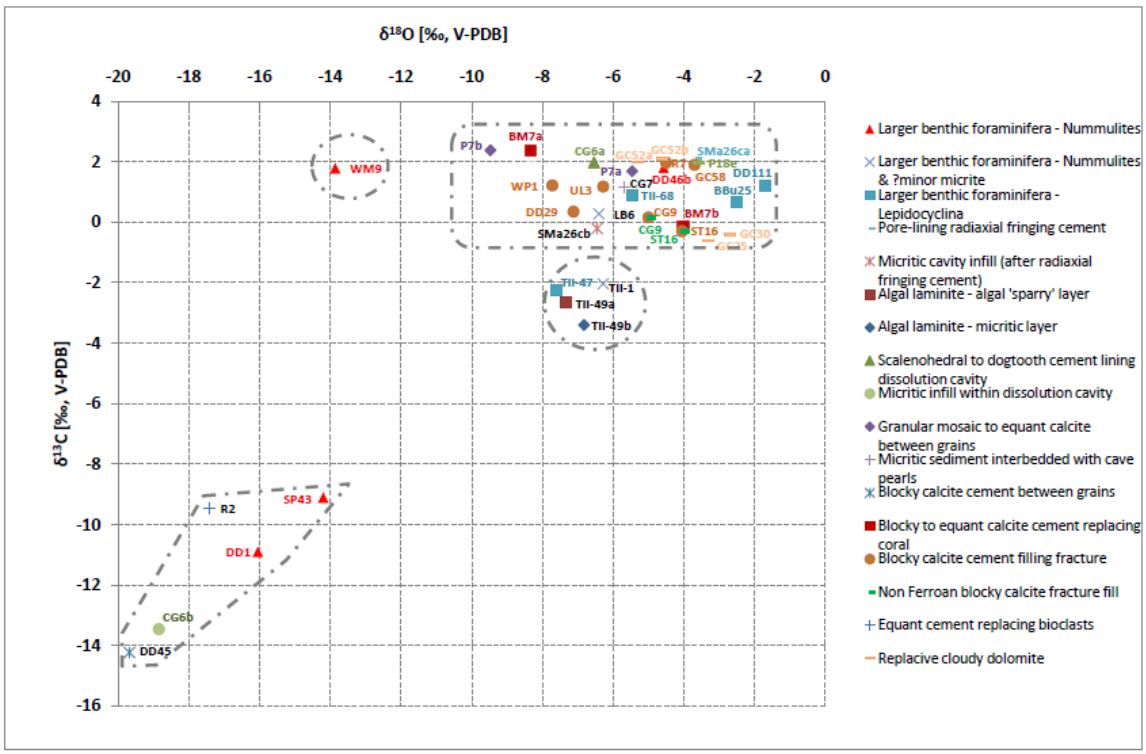

Figure 15

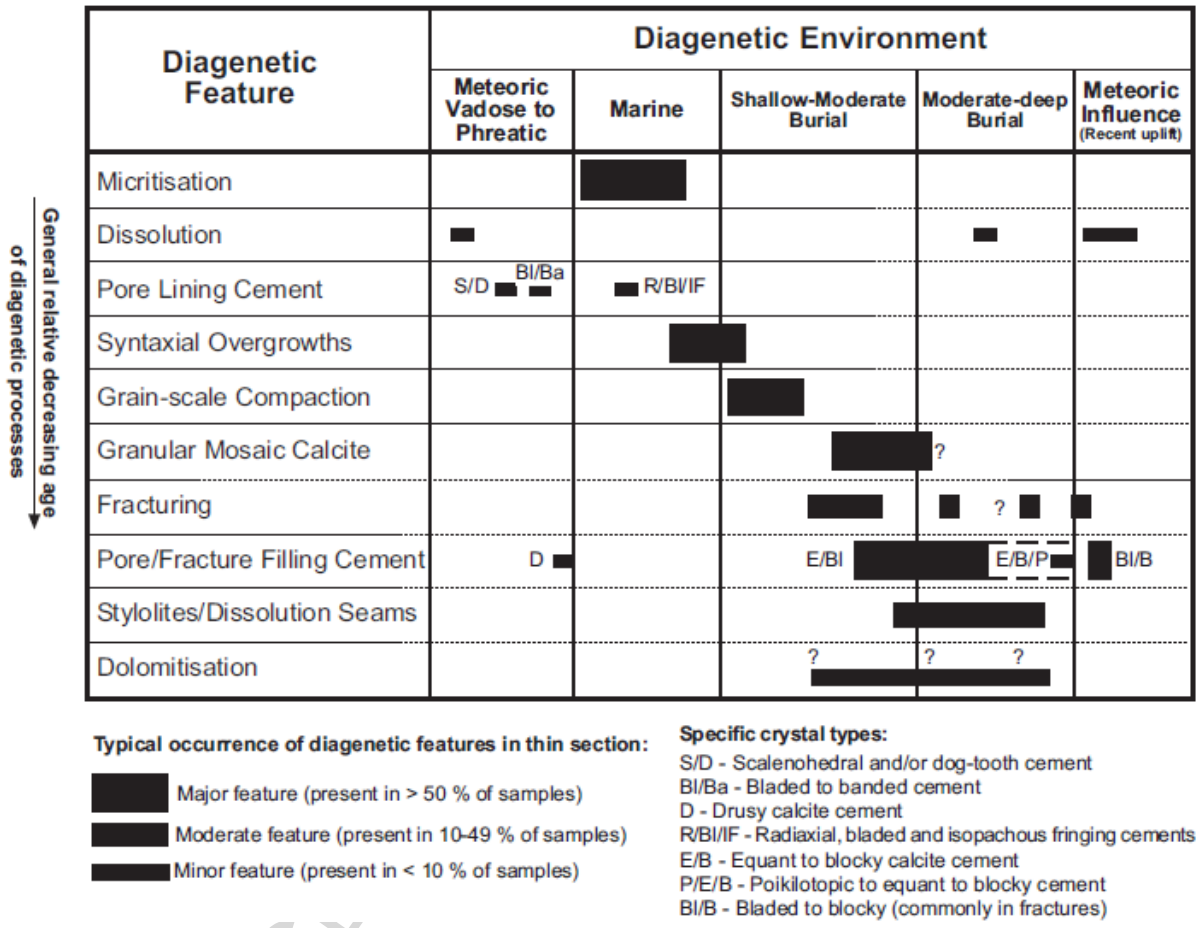

Figure 16